AWARD NUMBER: W81XWH-15-1-0306

TITLE: Predicting Sensitivity of Breast Tumors to Src-targeted Therapies Through Assessment of Cas/Src.BCAR3 Activity

PRINCIPAL INVESTIGATOR: Amy H. Bouton, PhD

CONTRACTING ORGANIZATION: University of Virginia
Charlottsville, VA 22904

REPORT DATE: October 2017

TYPE OF REPORT: Annual

PREPARED FOR: U.S. Army Medical Research and Materiel Command
Fort Detrick, Maryland 21702-5012

REPORT DOCUMENTATION PAGE

Form Approved
OMB No. 0704-0188

1. REPORT DATE	2. REPORT TYPE	3. DATES COVERED
October 2017	Annual	15 Sept 2016 – 14 Sept 2017

4. TITLE AND SUBTITLE
Predicting sensitivity of breast tumors to Src-targeted therapies through assessment of Cas/Src/BCAR3 activity

5a. CONTRACT NUMBER

5b. GRANT NUMBER
W81XWH-15-1-0306

5c. PROGRAM ELEMENT NUMBER

6. AUTHOR(S)
Amy H. Bouton, PhD

E-Mail: ahb8y@virginia.edu

5d. PROJECT NUMBER

5e. TASK NUMBER

5f. WORK UNIT NUMBER

7. PERFORMING ORGANIZATION NAME(S) AND ADDRESS(ES)

Rector and Visitors of the
University of Virginia

1001 N Emmett St.
Charlottesville, VA 22903-4833

8. PERFORMING ORGANIZATION REPORT NUMBER

9. SPONSORING / MONITORING AGENCY NAME(S) AND ADDRESS(ES)

U.S. Army Medical Research and Materiel Command
Fort Detrick, Maryland 21702-5012

10. SPONSOR/MONITOR'S ACRONYM(S)

11. SPONSOR/MONITOR'S REPORT NUMBER(S)

12. DISTRIBUTION / AVAILABILITY STATEMENT

Approved for Public Release; Distribution Unlimited

13. SUPPLEMENTARY NOTES

14. ABSTRACT

Purpose: The purpose of this research is to assess the role of a signaling pathway comprised of the protein tyrosine kinase c-Src (Src) and two adaptor molecules, Cas and BCAR3, in promoting breast tumor growth, metastasis and therapeutic resistance toward Src-targeted small molecule inhibitors.
Scope: The proposed research employs 2- and 3-dimensional tissue culture models, transplantable mouse models of breast cancer, and analysis of human breast tumor samples.
Major Findings: Key results from the second year of support include (1) BCAR3 protein expression is elevated in DCIS samples compared to normal mammary tissue, invasive ductal carcinoma (IDC) compared to normal mammary tissue, and DCIS compared to IDC. (2) BCAR3 is significantly upregulated in triple negative breast cancer and normal tissue; (3) BCAR3 expression shows a modest correlation to responsiveness to dasatinib in 2D culture; (4) BCAR3 expression regulates breast tumor initiation and growth in an MDA-MB-231 orthotopic tumor model; and (5) BCAR3 is required for mammary epithelial cells to activate appropriate growth factor signaling pathways that regulate mammary organoid development in 3D cultures.

15. SUBJECT TERMS
Breast tumor invasion, adhesion signaling, breast organoids, breast tumor initiation

16. SECURITY CLASSIFICATION OF:			17. LIMITATION OF ABSTRACT	18. NUMBER OF PAGES	19a. NAME OF RESPONSIBLE PERSON
a. REPORT	b. ABSTRACT	c. THIS PAGE			USAMRMC
U	U	U	UU	29	19b. TELEPHONE NUMBER *(include area code)*

Table of Contents

Page

1. INTRODUCTION

The goal of this project is to (1) understand the cooperating pathways through which signaling by the Cas/Src/BCAR3 signaling node drives tumor growth, metastasis and therapeutic resistance; and (2) be poised to begin clinical trials that will test BCAR3 expression as a predictor of response to the Src inhibitor dasatinib in combination with estrogen receptor (ER) and/or EGFR/HER2-targeted therapies. We continue to make good progress and achieve key milestones. We have BCAR3 expression is significantly upregulated in ductal carcinoma in situ (DCIS) and invasive breast cancers, independent of molecular subtype. We have shown that BCAR3 is required for tumor initiation in an orthotopic transplantable murine model of breast cancer, as well as being a key regulator of the growth of established tumors. These data provide support for the possibility of targeting pathways emanating from BCAR3 for the treatment of multiple subtypes of breast cancer in the clinic. We have developed a breast organoid system to specifically test the role for BCAR3 and the Cas/Src/BCAR3 signaling node and its interactions with EGFR family members in breast morphogenesis and tumor initiation. These accomplishments place us in an excellent position to continue along the strong trajectory of progress that has been achieved during this first two years of support.

Table 1. Clinical Breast Tissue Samples

Tumor Type	Number of Samples
DCIS	54
E+H+ IDC	13
ER+ IDC	51
H+ IDC	22
TN IDC	49
ER+PR- IDC	1
TOTAL	**190**
Normal	21

DCIS = Ductal carcinoma in situ;
IDC = Invasive ductal carcinoma;
ER = Estrogen receptor;
PR = Progesterone receptor;
H = HER2; TN = Triple-negative

2. KEY WORDS

Breast tumor invasions, adhesion signaling, breast organoids, breast tumor initiation.

3. ACCOMPLISHMENTS

Specific Aim 1; Task 1. (see revised SOW from year 1 progress report)

Specific Aim 1; Task 2. ***Expand the pilot study to evaluate BCAR3 expression in a larger cohort of clinical breast tumor samples.*** Two or three independent investigators (one pathologist and 1-2 researchers) have scored the breast tumor samples shown in **Table 1** for BCAR 3 expression and evaluated the analogous H&E stained tissue to identify possible defining features/architecture of regions of high BCAR3 expression (**Fig. 1**). Our biostatistician has analyzed these data to determine whether there is a correlation between BCAR3 expression and a particular subtype and/or grade of DCIS or invasive ductal carcinoma. By taking the average BCAR3 expression score across the entire tumor sample, BCAR3 protein expression was seen to be elevated in DCIS samples compared to normal mammary tissue, invasive ductal carcinoma (IDC) compared to normal mammary tissue, and DCIS compared to IDC (comparison of all three by Kurskal-Wallis test, individual pairs by the student T-test). However, there did not appear to be a statistically significant association between BCAR3 protein expression and tumor subtype based on ER/PR and HER2 expression.

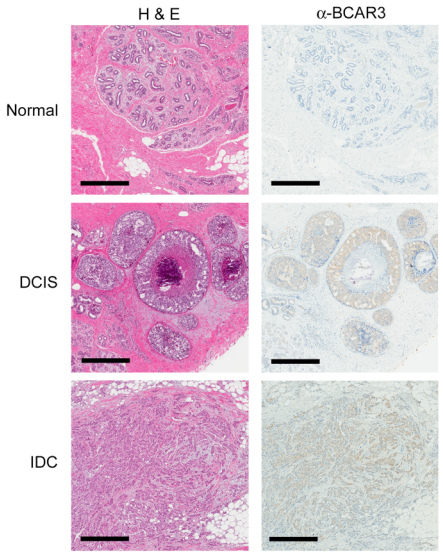

Fig. 1. BCAR3 expression is upregulated in DCIS and Invasive Ductal Carcinoma (IDC). Representative H&E and BCAR3-stained samples of mammary tissue/tumor obtained through the UVA Biorepository. Bar = 500 μm.

We then performed a preliminary analysis in two cohorts of Triple Negative Breast Cancers (TNBC) to determine whether BCAR3 is preferentially expressed in that subtype compared to normal breast tissue. We evaluated 17 formalin-fixed, paraffin-embedded TNBSs from the UVA tumor bank for the most intense

BCAR3 staining regions (**Fig. 2, top panels**) and found BCAR3 to be expressed at detectable levels in 16 of the tumors, with regions of 2+/3+ staining in 65% of the cases (**Fig. 2, bottom panels, black bars**). This is in contrast to normal breast tissue, whch exhibited 0 or 1+ staining in 100% of the samples (gray bars). We also stained a tumor microarray (TMA) generated by the UVA Department of Pathology from core biopsy materials (Dill *et al*., 2017. *Am J Surg Pathol* **41**:334-342). The TMA contained 40 individual TNBCs that showed variable levels of BCAR3 expression; 95% exhibited some BCAR3 expression and 69% exhibited regions of moderate/high (2+/3+) BCAR3 (data not shown). Together, these data provide the rationale for a more robust analysis of BCAR3 expression and signaling in TNBC subtypes.

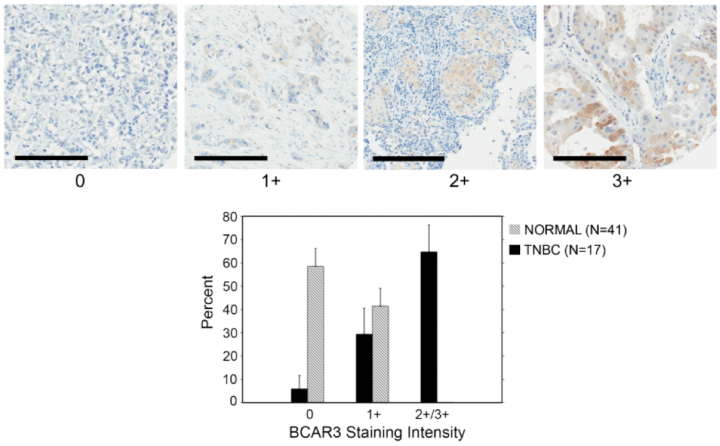

Fig. 2. BCAR3 expression is elevated in TNBCs compared to normal ductal mammary epithelium. Normal and TN invasive ductal carcinoma FFPE samples were stained for BCAR3 using a protocol validated by the Biorepository and Tissue Research Facility (BTRF) at UVA. (Top) Representative images from invasive carcinoma samples showing scoring for BCAR3 on a 0 to 3+ scale. Bar = 200 µm. (Bottom) The percentage of normal (gray bars) and TNBC (black bars) tissue samples containing regions of maximum BCAR3 staining intensity at the indicated levels. P<0.001, chi-squared test showing significant differences in BCAR3 expression between normal and TNBC tissues.

<u>Specific Aim 2; Task 3</u>. ***Determine whether dasatinib sensitivity can be modulated by BCAR3 expression and Cas/Src/BCAR3 signaling in tissue culture models.*** We continue to investigate whether BCAR3 expression levels impact sensitivity to Src inhibition by dasatinib. The rationale for these studies comes from strong biochemical data demonstrating elevated Src activity as a function of BCAR3 expression in breast cancer cells. Using a loss-of-function approach in two cell lines that express relatively high amounts of BCAR3, we have found a modest (~2-fold) increase in the IC50 for dasatinib in cells that express reduced amounts of BCAR3 (**Figs. 3A and 3B**). We performed a similar study using a gain-of-function model in MDA-MB-453 breast cancer cells, which typically express very low levels of BCAR3. In that case, we saw a modest very decrease in IC50 in the cells that overexpressed BCAR3 (**Fig. 3C**). Together, these data, coupled with our previous data showing a reduction in Src kinase activity when BCAR3 levels are depleted and an increase in Src activity when BCAR3 is overexpressed, indicate that BCAR3 expression levels may help predict response to Src inhibitors like dasatinib. However, because the BCAR3-dependent effects are so modest under 2D culture conditions, we plan to adapt these drug sensitivity studies to 3D culture systems, which have revealed robust functional deficiencies in cells depleted for BCAR3 (see Cross *et al*., 2016 provided in **Appendix 2** and organoid cultures shown below in **Fig. 6**).

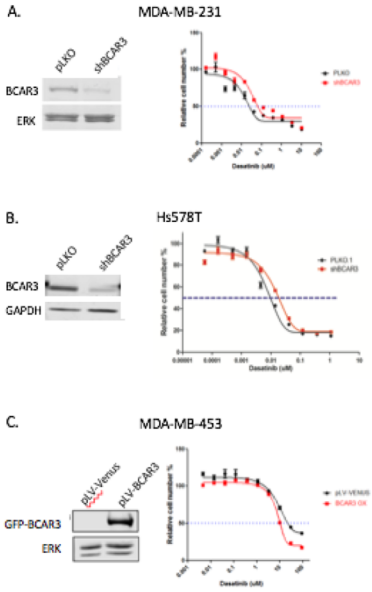

Fig. 3. Modulation of BCAR3 protein levels in 3 breast cancer cell lines has a modest effect on dastanib sensitivity. The indicated cell lines were stably transduced with constructs encoding shBCAR3 (panels A and B) or GFP-BCAR3 molecules. BCAR3 and control (ERK or GAPDH) protein levels for each cell line were measured by immunoblot (left panels). Cell viability was determined by MTT assays after 48 hours in the indicated concentrations of dasatinib.

<u>Specific Aim 2; Task 4.</u> ***Determine whether dasatinib sensitivity can be modulated by BCAR3 expression and Cas/Src/BCAR3 signaling in mouse models.*** As a first step in this aim, we sought to determine whether BCAR3 expression was required for primary tumor initiation or growth. Using an

orthotopic transplantable model, we reported in the 1st year progress report and more clearly herein that MDA-MB-231 breast cancer cells depleted for BCAR3 are significantly impaired in tumor initiation (**Fig. 4**). These data strongly implicate BCAR3 as a regulator of tumor initiation. We have since generated a cell line expressing a conditional knockdown allele for BCAR3 to investigate whether the growth of established tumors was similarly impacted under conditions of BCAR3 knockdown. Tumors were allowed to grow in the presence of BCAR3 until they reached 200 mm^3, after which the mice were fed doxycycline (Dox) in their drinking water to deplete BCAR3. The tumors continued to grow in animals injected with control cells (pLKO) and treated with Dox, while tumors established with the conditional shBCAR3 (shB3) cells failed to increase in size after Dox treatment was initiated (**Fig. 5A**). Tumors isolated from animals injected with cells transduced with the pLKO vector stained positively for BCAR3, while cells transduced with pLKO-shBCAR3 had markedly reduced levels of BCAR3 (**Fig. 5B**). We are now poised to investigate whether these tumors will show differential sensitivity to dasatinib as a function of BCAR3 expression.

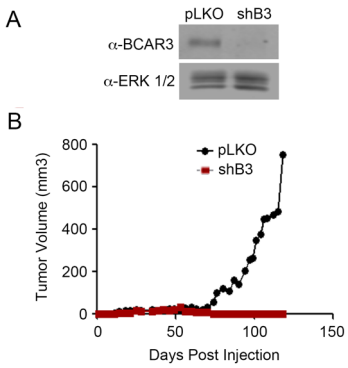

Fig. 4. BCAR3 regulates initiation/progression of MDA-MB-231 xenografts. 10^6 vector-controlled (pLKO) or BCAR3-depleted (shB3) MDA-MB-231 cells (see panel A) were implanted into the mammary fat pads of nude mice. (B) Tumors were measured by caliper 2-3 times per week for the indicated times. Data are the median for 7 pLKO and 8 shBCAR3 tumors. P<0.05, F-test from log-linear repeated measures model.

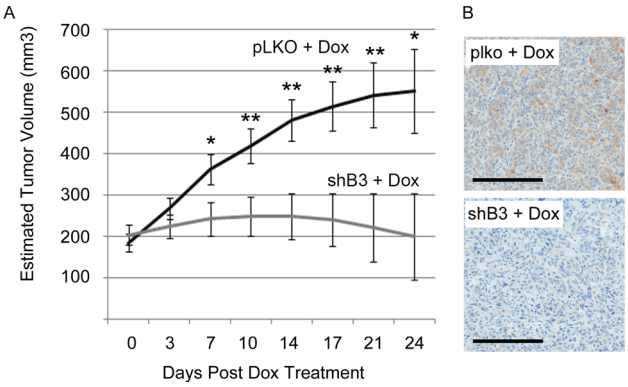

Fig. 5. BCAR3 regulates growth of MDA-MB-231 tumors in nude mice. (A) 10^6 Dox-inducible vector-controlled (pLKO) or BCAR3-depleted (shB3) MDA-MB-231 cells were implanted into the 4th mammary fat pad of nude mice. Once tumors reached ~200mm^3, the animals were fed Dox for the duration of the experiment. Tumors were measured by caliper 2-3 times per week. Data presented are the mean +/- SEM for 10 pLKO and 8 shBCAR3 tumors. Using quadratic mixed effect models, **P*<0.03 and ***P*<0.01. (B) Representative images of FFPE tumor sections stained for BCAR3. Bar = 200μm.

Specific Aim 3; Task 5. ***Test the hypothesis that Cas/Src/BCAR3 is downstream of HER family signaling in breast cancer cells using 2D and 3D systems.*** We have taken a somewhat different approach to testing this hypothesis than was proposed in the initial grant due to having obtained global BCAR3 knockout (KO) mice from our collaborator, Dr. Adam Lerner (Boston University). Using these mice, we generated mammary organotypic cultures ("organoids") from epithelium isolated from the mammary glands of wildtype and BCAR3 KO mice. Wildtype mammary epithelial cells form polarized glandular structures when cultured in a laminin-rich matrix such as matrigel and produce bud-like structures through a process similar to branching morphogenesis in the presence of FGF2 (**Fig. 6, top left**) and EGFR family ligands such as transforming growth factor α (TGFα) (**top right**) and neuregulin (data not shown). This requires complex growth factor responses, cell-cell and cell-matrix interactions, and tissue remodeling, all of which can be de-regulated during tumorigenesis. As a consequence, mammary organoid cultures afford a powerful tool to

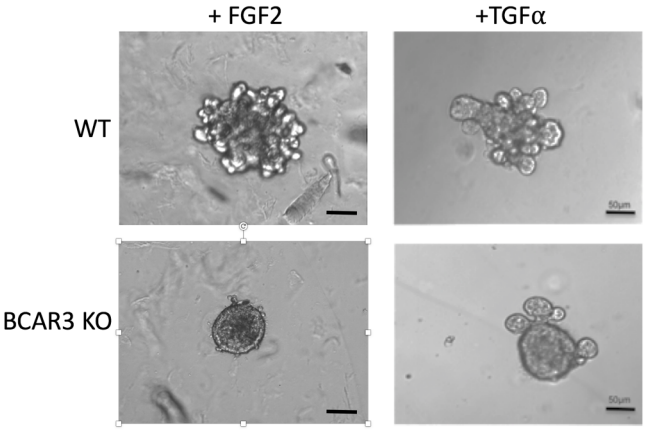

Fig. 6. BCAR3 regulates organoid branching. Cells were isolated from WT or BCAR3 KO mice, dispersed, and plated in matrigel in the presence or absence of 2 nM FGF2 (left) or 9 nM TGFα (right).

interrogate cellular mechanisms that contribute to breast tumorigenesis. We showed during our previous progress report that mammary organoids generated from global BCAR3 KO mice failed to undergo significant branching in response to FGF2 (**Fig. 6, bottom left**), and more recently we found that the same was the case when BCAR3 KO cells were treated with the EGFR ligand TGFα (**bottom right**), showing that mammary epithelial cells are unable to activate appropriate growth factor signaling networks to promote branching in the absence of BCAR3. Based on these robust phenotypes, we believe that this system will be a powerful tool for identifying the molecular pathways through which EGFR family members functionally and physically interact with BCAR3. We are currently measuring activation of signaling molecules downstream of EGFR family members (e.g. ERK and AKT), proliferation markers (e.g. pRB, ki67, cyclin D1), and basal/luminal polarity markers (cytokeratins 5/6 and 18, respectively) to define BCAR3-EGFR family networks.

Specific Aim 3; Task 6. No progress to date.

Research Team Meetings. The research team has met both as a group and in smaller units frequently to discuss data acquisition, analysis, and future directions.

4. IMPACT

While Src inhibitors have shown some activity in breast cancer patients, their lack of consistent efficacy has been somewhat surprising in light of the fact that elevated Src activity is a feature of many breast cancers. Nonetheless, Src inhibitors continue to be considered as potentially viable options for the treatment of breast cancer, largely because Src activity has been implicated in tumor and tumor cell behaviors associated with proliferation, survival, invasion, metastasis, and therapeutic resistance. Thus, there is a desperate need for new approaches that can guide their application to patients who will most likely benefit from this class of drugs. With the extensive collection of clinical breast tumor samples that we have examined (**Table 1, Figs. 1** and **2**); the robust phenotypes that we have identified demonstrating a role for BCAR3 in tumor initiation/growth (**Figs. 4** and **5**); organoid branching (**Fig. 6**); and invasion (Cross *et al.,* 2016); the genetic and cellular tools that we have developed; and the combined expertise of our team, we will be well positioned to rapidly translate this work into the clinic and thus provide benefit to these patients.

5. CHANGES/PROBLEMS

Specific Aim 3. ***Investigate the role of Cas/Src/BCAR3 in EGFR/HER2 signaling and response to targeted therapies***. Evidence for a functional connection between BCAR3 and EGFR family members has come from a recent article by Li *et al.* (2017. *Nature Cell Biology* **19**:106-119), who reported that the SH2 domain of BCAR3 mediates direct binding to human epidermal growth factor receptor 3 (HER3), which recruits a second receptor-like tyrosine kinase (ROR1) and activates downstream YAP transcriptional programs. These investigators showed that this pathway was activated by the HER3 ligand neuregulin, leading to activation of HER2/HER3 heterodimers and downstream signaling. Using the 3D organoid culture described above, we will begin to explore whether this pathway plays a key role in BCAR3 activities involved in growth factor signaling, cell polarity, and proliferation. We will also begin to assess the degree of integration required between BCAR3 and EGFR or HER3 pathways by assessing the level of activation of the receptors and downstream signaling molecules in the tumors generated for Aim 2, Task 4 as a function of BCAR3 expression. While the functional domains on BCAR3 required to couple with EGFR signaling are not known, comparisons between tumor phenotypes elicited by cells re-expressing WT BCAR3 and cells expressing the SH2-deficient BCAR3 variant (BCAR3-R177K) that does not bind to HER3 will help to determine whether interactions between BCAR3 and HER3 are required for BCAR3-dependent tumorigenesis. Finally, we are using in vitro 3D models to identify changes in transcriptional programs as a function of BCAR3 expression.

6. PRODUCTS

The following paper has now been published (November 10, 2016): Cross, AM, Wilson, AL, Guerrero, MS, Thomas, KS, Bachir, AI, Kubow, KE, Horwitz, AR, and Bouton, AH. 2016. Breast cancer antiestrogen resistance 3-p130^{Cas} interactions promote adhesion disassembly and invasion in breast cancer cells. *Oncogene* **35**:5850-5859. (see **Appendix 2**)

7. PARTICIPANTS AND OTHER COLLABORATING ORGANIZATIONS

Participant	Role	Salary Support
Amy H. Bouton, Ph.D.	Principal Investigator	Unchanged
Kristen Atkins, M.D.	Co-Investigator	Unchanged
Mark Conaway, Ph.D.	Co-Investigator	Unchanged
Patrick Dillon, M.D.	Co-Investigator	Unchanged
Carol Gold, J.D., LLM	Consumer Advocate	Unchanged
Barbara Dziegielewska	Research Scientist	3.09%
Ryan Llewellyn	Graduate Research Assistant	100%
Keena Thomas, M.S.	Laboratory Specialist	95%

Other support: Please see the revised "Other Support" documents for Drs. Conaway and Dillon (**Appendix 1**).

8. SPECIAL REPORTING REQUIREMENTS – None to report.

9. LIST OF APPENDICES

- **Appendix 1.** Revised "Other Support" for Drs. Conaway and Dillon (pages 9-12).
- **Appendix 2**. Cross *et al.,* 2016. Breast cancer antiestrogen resistance 3-p130^{Cas} interactions promote adhesion disassembly and invasion in breast cancer cells. *Oncogene* **35**:5850-5859.

OTHER SUPPORT

CONAWAY, M.

ACTIVE

R01CA142859-04A1 (Conaway) **05/01/2014-04/30/2018** **2.7 calendar**
NIH/NCI
Designs for phase I trials in heterogeneous groups
The goal of this project is to develop and test statistical designs for dose-finding trials conducted in heterogeneous groups of patients.

P30CA044579-23 (Loughran) **02/01/2017-01/31/2022** **0.6 calendar**
NIH/NCI
Cancer Center Support Grant (Biostatistics Core)
Role: Co-investigator
This is to support investigators in the UVA Cancer Center in the design and analysis of studies related to cancer.

R01HD068345-02 (Ramey/Stevenson/Case-Smith) **09/27/2012-07/30/2017** **1.2 calendar**
NIH/NICHHD
Multi-Site RCT of Pediatric Constraint-Induced Movement therapy (CIMT)
Role: Co-investigator
The proposed study is a multi-site, randomized controlled trial (RCT) of 144 children (3 - 6 yrs old) with hemiparetic CP

K24AI102972-02 (Houpt) **07/01/2013-06/30/2018** **0.78 calendar**
NIH/NIAID
Molecular Diagnostic Tools for Patient-Oriented Field Studies in ID
Role: Co-investigator
The goal of this project is to develop patient-oriented studies in order to inform clinically important areas such as the cause of diarrhea in developing countries and proper treatment for MDR Tb.

R01CA178338-01A1 (Gioeli) **05/01/2014-04/30/2019** **0.6 calendar**
NIH/NCI
Checkpoint Signaling and Androgen Receptor Function in Prostate Cancer
Role: Co-investigator
This project seeks to determine the mechanism of CHK2 regulation of AR activity and CRPC cell growth.

P01HL120840-01A1 (Ravichandran) **08/01/2014-05/31/2019** **0.6 calendar**
NIH/NHLBI
Role of pannexins in vascular physiology and inflammation
Role: Co-investigator
This project comprises several research projects surrounding the role of pannexin in vascular physiology. My specific role will be to assist with biostatistical issues in the design and analysis of experiments.

BC141713 (Bouton) **9/15/15-9/14/18** **0.36 calendar**
DOD Breast Cancer Research Program
Predicting sensitivity of breast tumors to Src-targeted therapies through assessment of Cas/Src/BCAR3 activity.
CURRENT PROPOSAL

1R01HL121635-01A1 (Annex) **07/01/2015-06/30/2018** **(0 cal this year)**
NIH
MicroRNA in Peripheral Arterial Disease
Role: Co-investigator
This project uses in vitro and in vivo experiments to investigate the role of miR-93 in PAD.

1U01NS088034-01 (Kapur) **09/30/2014-02/29/2020** **0.12 calendar**
NIH
Established Status Epilepticus Treatment Trial (ESETT)
Role: Co-investigator
This is a multi-site randomized clinical trial of 3 current treatments in epliepsy: fosphenytoin, levetiracetam and valproic acid.

1R01HL128492-01A1 (Lau) **04/12/2016-03/31/2021** **1.2 calendar**
NIH
Prevention of lung transplant injury with adenosine 2a receptor agonist
Role: Co-investigator
This is a phase I, dose-finding clinical trial of an adenosine 2a receptor agonist.

R01 (Cox) **07/01/2016-06/30/2020** **1.2 calendar**
NIH
Treating type 2 diabetes by reducing postprandial glucose elevations: A paradigm shift in lifestyle modification
Role: Co-investgator
This is a randomized trial of 4 behavioral interventions for the treatment of type II diabetes.

R01 (Salerno) **09/01/2016-08/31/2020** **0.6 calendar**
NIH
High-Resolution Whole Heart Quantitative CMR Perfusion Imaging in Ischemic Heart Disease
Role: Co-investigator
This project investigates the use of high resolution imaging in diagnosing ichemic hearty disease.

OPP1141342 (Mduma) **11/17/2016-11/30/2019** **0.12 calendar**
Bill and Melinda Gates Foundation
ELICIT: Early Life Interventions for Childhood Growth and Development In Tanzania
Major goals of the project: Using a factorial design, test interventions of administering antimicrobials and nicotinamide among children 0-18 months old, measuring outcomes of linear growth, intestinal infection and child cognitive development.

Overlap
There is no scientific or budgetary overlap with any of these projects and the current grant.

PENDING

R01 (Lazo) **11/01/2017-10/31/2021** **0.24 calendar**
PTP4A3 Phosphatase and Colorectal Cancer
NIH
Role: Co-investigator
This project proposes to elucidate the function of a tyrosine phosphatase PTP4A3 using a small molecule approach and validate PTP4A3 as a therapeutic target in colorectal disease.

R33 (Gioeli) **01/01/2018-12/31/2020** **.24 calendar**
NIH-NCI
Validation of the Pancreatic Cancer Tumor Microenvironment System (TMeS) for drug discovery and personalized medicine
Role: Co-investigator
This project examines the role of the pancreatic tumor microenvironment.

OTHER SUPPORT

DILLON, PATRICK M.

ACTIVE

U.S. Dept of Defense - Army Medical Command (Bouton), Dillon (Sub-Investigator) 9/15/15-9/14/18
GG11879/149747 0.24 cal mos. *"Predicting Sensitivity of Breast Tumors to Src-targeted Therapies Through Assessment of Cas/Src/BCAR3 Activity"*
This project will seek to develop methods to determine which tumors will respond to a given drug and which combinations of drugs will produce the most benefit for the patient. This requires detailed knowledge of the intracellular signaling pathways that drive tumor growth and metastasis in specific tumor subtypes. In this proposal, we focus on a signaling network comprised of three proteins, the adapter molecules $p130^{Cas}$ (Cas) and Breast Cancer Antiestrogen Resistance-3 (BCAR3), and the tyrosine kinase c-Src (Src). The rationale for concentrating on this signaling node stems from extensive data in support of these molecules controlling tumor cell proliferation, survival, invasion, tumor growth, metastasis, and therapeutic response. The project thus addresses two overarching challenges: 1) Identify what drives breast cancer growth: determine how to stop it and 2) Eliminate the mortality associated with metastatic breast cancer. (CURRENT GRANT)

U.S. Dept of Defense - Army Medical Command (Dzielgewski), Dillon (Sub-I) 9/15/15-9/14/18
GG11882/149829 0.36 cal mos. *"Low-Voltage Activated Calcium Channels - Their Role in HER2-Driven Breast Cancer and Potential as a New Therapeutic Target"*
This project focuses on the role of low voltage activated calcium channels (LVA, also called T-type channels) in breast cancer development, progression and resistance to therapy. Preliminary results suggest that overexpression/aberrant activation of LVA channels is an important pro-survival and anti-therapy mechanism for breast cancer, especially for the subtype overexpressing human epidermal growth factor receptor 2 (HER2+). Therefore, the study of LVA channels may identify what drives breast cancer growth and determine how to stop it. Importantly, an efficient, safe, and clinically available inhibitor of LVA channels, mibefradil, is currently being developed as anti-cancer agent and will be studied in mouse models in this project with plans to translate results to a future clinical trial at the University of Virginia. (NO OVERLAP)

Focused Ultrasound Foundation (Dillon) 7/1/2017-6/30/2019 1 cal mos.
SR00211/153117
"Focused Ultrasound Therapy to Augment Antigen Presentation and Immune-Specificity of Checkpoint Inhibitor Therapy with Pembrolizumab for Metastatic Breast Cancer"
The goal of this project is to test whether partial tumor ablation via focused ultrasound energy delivery might augment antigen presentation and improve systemic response to PD-1 inhibitor therapy with the drug pembrolizumab. This is a phase I clinical trial with correlative immunologic evaluations. (NO OVERLAP)

PENDING

None

OVERLAP

There is no scientific or budgetary overlap with any of these projects.

Oncogene (2016) **35**, 5850–5859

www.nature.com/onc

ORIGINAL ARTICLE

Breast cancer antiestrogen resistance 3 – p130^{Cas} interactions promote adhesion disassembly and invasion in breast cancer cells

AM Cross[1,5], AL Wilson[1,5], MS Guerrero[2], KS Thomas[1], AI Bachir[3], KE Kubow[4], AR Horwitz[3] and AH Bouton[1]

Adhesion turnover is critical for cell motility and invasion. We previously demonstrated that the adaptor molecule breast cancer antiestrogen resistance 3 (BCAR3) promotes adhesion disassembly and breast tumor cell invasion. One of two established binding partners of BCAR3 is the adaptor molecule, p130^{Cas}. In this study, we sought to determine whether signaling through the BCAR3–Cas complex was responsible for the cellular functions of BCAR3. We show that the entire pool of BCAR3 is in complex with Cas in invasive breast tumor cells and that these proteins colocalize in dynamic cellular adhesions. Although accumulation of BCAR3 in adhesions did not require Cas binding, a direct interaction between BCAR3 and Cas was necessary for efficient dissociation of BCAR3 from adhesions. The dissociation rates of Cas and two other adhesion molecules, α-actinin and talin, were also significantly slower in the presence of a Cas-binding mutant of BCAR3, suggesting that turnover of the entire adhesion complex was delayed under these conditions. As was the case for adhesion turnover, BCAR3–Cas interactions were found to be important for BCAR3-mediated breast tumor cell chemotaxis toward serum and invasion in Matrigel. Previous work demonstrated that BCAR3 is a potent activator of Rac1, which in turn is an important regulator of adhesion dynamics and invasion. However, in contrast to wild-type BCAR3, ectopic expression of the Cas-binding mutant of BCAR3 failed to induce Rac1 activity in breast cancer cells. Together, these data show that the ability of BCAR3 to promote adhesion disassembly, tumor cell migration and invasion, and Rac1 activity is dependent on its ability to bind to Cas. The activity of BCAR3–Cas complexes as a functional unit in breast cancer is further supported by the co-expression of these molecules in multiple subtypes of human breast tumors.

Oncogene (2016) **35,** 5850–5859; doi:10.1038/onc.2016.123; published online 25 April 2016

INTRODUCTION

Cell motility is an essential feature of processes involved in development and tissue repair, as well as in pathological states such as inflammation and cancer. A signaling node comprised of the adaptor molecules breast cancer antiestrogen resistance 3 (BCAR3) and p130^{Cas} (Cas; also known as BCAR1) has been established as a regulator of several aspects of motility, including cell protrusion, adhesion, migration and invasion.[1–5] BCAR3 is a member of the novel SH2 domain-containing protein (NSP) family of adaptor molecules, and contains an N-terminal SH2 domain and a C-terminal guanine nucleotide exchange factor (GEF)-like domain with sequence homology to the Cdc25 family of Ras GEFs.[6–8] These domains promote the interaction between BCAR3 and its two established binding partners, protein tyrosine phosphatase α and Cas, respectively.[3,9] Cas contains multiple protein interaction domains that contribute to its localization to focal adhesions and its activity as a regulator of cell motility.[10]

BCAR3 and Cas bind directly to one another at their C-termini. The C-terminal domain of BCAR3 adopts a 'closed' conformation, which is not only necessary for its binding to Cas but also prevents the C-terminus of BCAR3 from functioning as a GEF.[9] BCAR3 association with Cas has been shown to stabilize each protein and enhance Cas–c-Src (Src) interactions, Src kinase activity and Src-mediated Cas tyrosine phosphorylation.[3,5,11]

Previous work from our group and others showed that BCAR3 promotes migration and invasion in breast cancer cell lines.[2,4] One of the first steps in cell migration is the formation of nascent adhesions at the leading edge of a migrating cell.[12] These nascent adhesions can either undergo disassembly (turnover) or they mature into focal complexes and focal adhesions. Adhesion turnover is initiated when there is a lack of tension to reinforce the adhesion. This is mediated through adaptor molecules and kinases that function in adhesions to locally activate Rac1 and inhibit RhoA GTPase signaling, thereby reducing tension and promoting adhesion disassembly.[13,14] In order for the cell to move forward, adhesions in the rear of the cell must also undergo disassembly. We have previously demonstrated that the adaptor molecule BCAR3 promotes Rac1 activity and adhesion disassembly in invasive breast cancer cells.[4] However, the mechanism(s) through which BCAR3 contributes to these activities remained to be elucidated.

In this study, we sought to determine the role of the BCAR3–Cas complex in BCAR3-mediated adhesion dynamics, migration and invasion of breast cancer cells. We found that all of the BCAR3 in invasive breast cancer cells is present in a complex with Cas and

[1]Department of Microbiology, Immunology and Cancer Biology, University of Virginia School of Medicine, Charlottesville, VA, USA; [2]Fujifilm Diosynth Biotechnologies, USA, Inc., Cary, NC, USA; [3]Department of Cell Biology, University of Virginia School of Medicine, Charlottesville, VA, USA and [4]Department of Biology, James Madison University, Harrisonburg, VA, USA. Correspondence: Dr AH Bouton, Department of Microbiology, Immunology and Cancer Biology, University of Virginia School of Medicine, Box 800734, Charlottesville, VA 22908, USA.
E-mail: ahb8y@virginia.edu
[5]These authors contributed equally to this work.
Received 30 July 2015; revised 10 February 2016; accepted 7 March 2016; published online 25 April 2016

that both proteins colocalize in focal adhesions. BCAR3 entry into adhesions did not require a direct interaction with Cas or an intact SH2 domain. However, the kinetics of BCAR3 dissociation from adhesions was impaired in the absence of Cas binding. This paralleled a similar delay in the dissociation of other adhesion proteins, indicating that BCAR3–Cas interactions have an important role in adhesion complex disassembly. The BCAR3–Cas complex was also found to be important for BCAR3-dependent Rac1 activation, migration and invasion in three-dimensional (3D) matrices. Finally, BCAR3 and Cas were found to be co-expressed in multiple subtypes of human breast tumors. Collectively, these data highlight the importance of a functional BCAR3–Cas complex in invasive breast cancer cells.

RESULTS

The entire cellular pool of BCAR3 is in complex with Cas in invasive breast cancer cells

Given the evidence of a strong functional relationship between BCAR3 and Cas, we measured the steady-state levels of BCAR3–Cas complexes in invasive breast cancer cells. Lysates from BT549 and MDA-MB-231 cells were subjected to serial immunoprecipitations with either Cas or BCAR3 antibodies (Figure 1). BCAR3 was present in Cas immune complexes (Figure 1a, lanes 5–6 and 12–13) and coincidentally lost from the lysates following immune depletion of Cas (lanes 2–4 and 9–11), indicating that the majority of BCAR3 present in BT549 and MDA-MB-231 cells is in complex with Cas. In contrast, although Cas was also present in BCAR3 immune complexes (Figure 1b, lanes 5 and 12), significant amounts of Cas remained in the lysates following immune depletion of BCAR3 (lanes 2–4 and 9–11). Together, these data show that, although a substantial pool of Cas is free of BCAR3, the majority of BCAR3 in invasive breast cancer cells is in complex with Cas. Based on these dynamics, it is likely that the interaction between these molecules is critical for the biological functions of BCAR3.

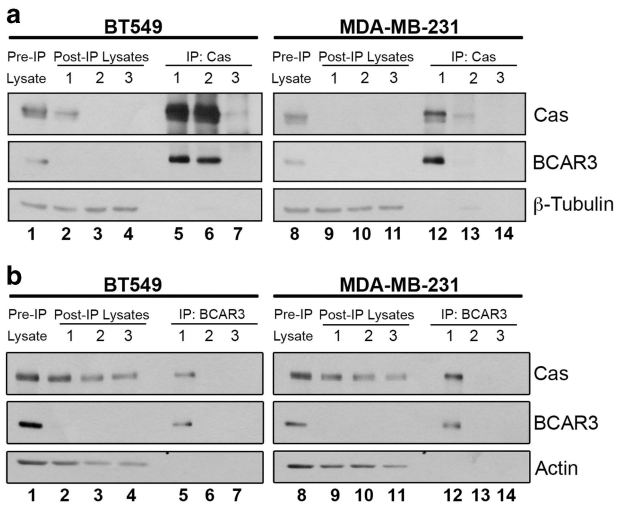

Figure 1. The entire cellular pool of BCAR3 is in complex with Cas. BT549 and MDA-MB-231 cell lysates were subjected to three serial Cas (**a**) or BCAR3 (**b**) immunoprecipitations (IP). Pre-IP lysates were separated by 8% sodium dodecyl sulfate–polyacrylamide gel electrophoresis (lanes 1 and 8) together with the proteins present in the IPs (lanes 5–7 and 12–14) and post-IP lysates (2–4 and 9–11). Proteins were immunoblotted with antibodies recognizing the designated proteins. The pre-IP lysate is 10% of the amount of protein used for the initial IP.

Localization of BCAR3 to adhesions does not require a functional SH2 domain or direct interaction with Cas

As discussed above, BCAR3 and Cas have substantial roles in motility and invasion. BCAR3 has been reported to localize to vinculin-containing adhesions in mouse embryo fibroblasts.[3] To determine whether BCAR3 also localizes to adhesions in human breast cancer cells, GFP-BCAR3 was expressed in BT549 invasive breast cancer cells and adhesions were visualized by total internal reflection fluorescence (TIRF) microscopy. Similar to mouse embryo fibroblasts, GFP-BCAR3 was present in adhesions in BT549 cells (Figure 2A, panel a). In addition, GFP-BCAR3 colocalized with endogenous Cas in these adhesions (panels a–c).

To determine which domains of BCAR3 are required for localization to adhesions, we generated functional domain mutants and expressed them in BT549 cells (Figure 2B). As the SH2 domain was previously demonstrated to be critical for BCAR3 localization to adhesions in mouse embryo fibroblasts,[3] we first investigated whether a mutant of this domain (R171V GFP-BCAR3) could localize to adhesions in breast cancer cells. This molecule was found to be present in adhesions and, like WT BCAR3, it colocalized with endogenous Cas (Figure 2A; panels d–f). This shows that the SH2 domain of BCAR3 is not the sole determinant of adhesion targeting in breast cancer cells. As a direct interaction between BCAR3 and Cas was reported to be important for their reciprocal stability,[5] and all of the BCAR3 in these cells is bound to Cas (Figure 1), we next asked whether localization of BCAR3 to adhesions requires association with Cas. This was addressed using a BCAR3 molecule containing two point mutations, L744E and R748E, which were recently shown to prevent the interaction between BCAR3 and Cas.[5] To verify that these point mutations abrogated Cas binding, Cas immune complexes were isolated from BT549 cells expressing WT GFP-BCAR3 or L744E/R748E GFP-BCAR3 (Figure 2B). As expected, endogenous BCAR3 (lower bands in lower panel, lanes 6–10) and WT GFP-BCAR3 (upper band, lane 7) were present in Cas immune complexes. However, L744E/R748E GFP-BCAR3 (L/R) failed to interact with Cas (lane 9). Despite the fact that this mutant was unable to bind to Cas, it was present in adhesions and colocalized with endogenous Cas (Figure 2A, panels g–i). This demonstrates that BCAR3 localization to adhesions does not require direct association with Cas.

Although neither the SH2 domain nor the Cas-binding domain were found to be solely responsible for BCAR3 localization to adhesions, these data do not discount the possibility that both domains could contain adhesion-targeting activity. To test this, a triple BCAR3 mutant (R171V/L744E/R748E GFP-BCAR3) that lacks both a functional SH2 domain and the Cas-binding site was expressed in BT549 cells. This molecule failed to associate with Cas (Figure 2B, lane 10); however, as was the case for the individual mutants, the triple mutant was present in adhesions and colocalized with Cas (Figure 2A, panels j–l). Together, these data show that, although protein tyrosine phosphatase α (through the SH2 domain) and/or Cas (through the C-terminus) may facilitate BCAR3 localization to adhesions, other mechanisms must be available in the absence of these interactions to recruit BCAR3 to adhesion sites in breast cancer cells.

Direct interaction between BCAR3 and Cas is required for efficient adhesion disassembly in BT549 breast cancer cells

Although BCAR3 localization to adhesions does not require a direct association with Cas, BCAR3 function may be dependent on this interaction. In a previous study, we demonstrated that BCAR3 promotes adhesion disassembly in invasive breast cancer cells.[4] To test whether this function is dependent on BCAR3–Cas interactions, live TIRF imaging was performed on BT549 cells that were co-transfected with plasmids encoding mCherry-tagged Cas and either WT or L744E/R748E GFP-BCAR3. Under these conditions, both WT and L744E/R748E GFP-BCAR3 colocalized with Cas in

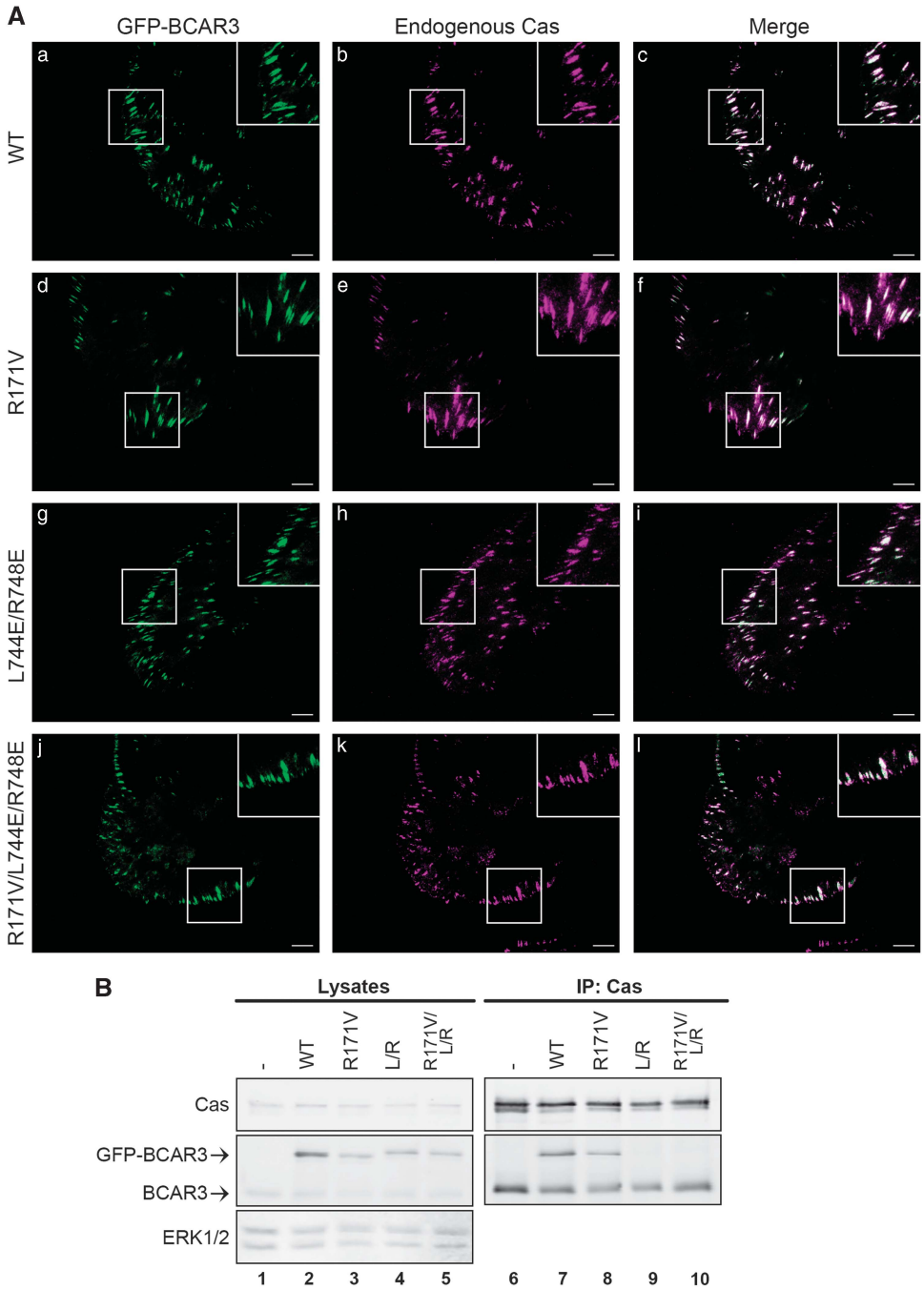

Figure 2. BCAR3 localization in adhesions does not require a functional SH2 domain or interaction with Cas. (**A**) BT549 cells were transfected with plasmids encoding WT GFP-BCAR3, R171V GFP-BCAR3, L744E/R748E GFP-BCAR3 or R171V/L744E/R748E GFP-BCAR3. Cells were incubated for 24 h before plating on 10 μg/ml fibronectin-coated coverslips for 4 h. Cells were fixed, stained with polyclonal Cas antibodies (panels b, e, h and k), and subjected to TIRF microscopy to visualize adhesions. Merged images are shown in the right panels and insets show higher magnifications of the designated areas. (**B**) BT549 cells were transfected with plasmids encoding GFP, WT GFP-BCAR3, R171V GFP-BCAR3, L744E/R748E GFP-BCAR3 or R171V/L744E/R748E GFP-BCAR3 and lysed in a non-denaturing buffer 24 h post transfection. Total cell protein and Cas immune complexes (generated from 50X more protein than the lysates) were immunoblotted with antibodies to detect the indicated proteins. Left and right panels are identical exposures from the same film.

dynamic adhesions (Figure 3). To quantify adhesion turnover, adhesions at peripheral, protruding edges of a cell were selected for analysis. Time-lapse images show incorporation (arrowheads) and dissociation (arrows) of BCAR3 and Cas into and from representative adhesions co-expressing Cas and either WT (Figure 3a) or L744E/R748E GFP-BCAR3 (Figure 3b). By measuring fluorescence intensity over time (Figures 3c and d), BCAR3 and Cas were found to incorporate into adhesions at similar rates (Figure 3e, compare bars 1 and 3). This was independent of the ability of BCAR3 to bind to Cas, as L744E/R748E GFP-BCAR3 entered adhesions at a rate similar to that of WT BCAR3 (compare bars 1 and 2). Moreover, when Cas was co-expressed with mutant BCAR3, it entered adhesions at a similar rate to when it was co-expressed with WT GFP-BCAR3 (compare bars

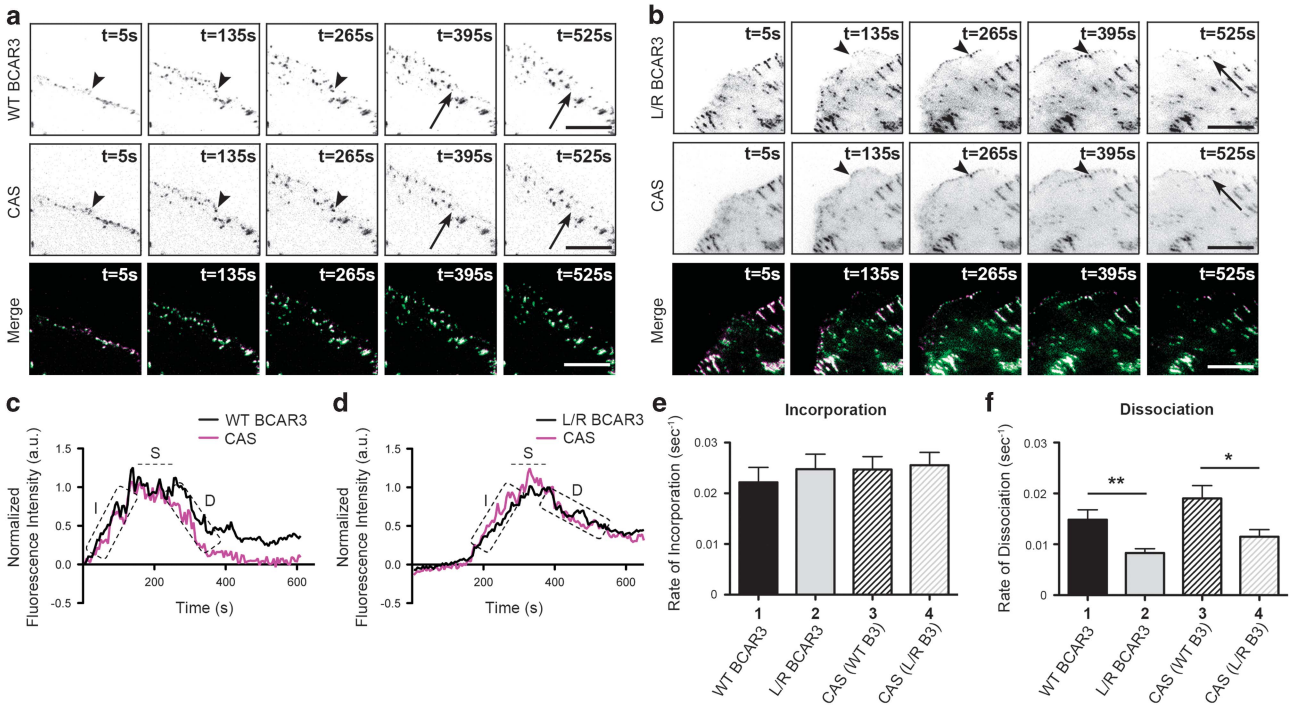

Figure 3. Direct interaction between BCAR3 and Cas is required for efficient dissociation of BCAR3 from adhesions. BT549 breast cancer cells were co-transfected with plasmids encoding WT or L744E/R748E (L/R) GFP-BCAR3 and mCherry-Cas, incubated for 24 h, and then plated on 2 μg/ml fibronectin-coated glass-bottomed TIRF dishes for 30–40 min before visualizing adhesion dynamics via live-imaging TIRF microscopy. (**a**, **b**) Representative time-lapse images show incorporation into adhesions (arrowheads) and dissociation (arrows) of the indicated proteins over the specified time course. Scale bars = 100 μm. (**c**, **d**) Representative fluorescence intensity time tracings of BCAR3 (black) and Cas (magenta) present in adhesions from cells expressing WT (**c**) or L744ER748E (**d**) GFP-BCAR3. Dashed boxes/line indicate the incorporation (I), stability (S) and dissociation (D) phases of adhesion dynamics. (**e**, **f**) Quantitative analysis of the incorporation (**e**) and dissociation (**f**) rates of WT GFP-BCAR3 (bar 1), L744E/R748E (L/R) GFP-BCAR3 (bar 2), Cas co-expressed with WT GFP-BCAR3 (bar 3), and Cas co-expressed with L744E/R748E (L/R) GFP-BCAR3 (bar 4). Data presented are the mean ± s.e.m. of ⩾35 adhesions from three WT and L744E/R748E GFP-BCAR3 expressing cells from three independent experiments. $^{*}P < 0.05$, $^{**}P < 0.01$.

3 and 4). Together, these data demonstrate that BCAR3 can efficiently incorporate into adhesions without being directly bound to Cas.

Using a similar approach to measure adhesion disassembly, we found that BCAR3 and Cas dissociate from adhesions at similar rates (Figure 3f, compare bars 1 and 3). However, the rate of L744E/R748E GFP-BCAR3 dissociation was significantly reduced compared with WT GFP-BCAR3 (compare bars 1 and 2), and dissociation of Cas from these adhesions was similarly impaired (compare bars 3 and 4). This suggests that direct binding between BCAR3 and Cas is required for efficient dissociation of BCAR3 and Cas from adhesions.

The reduced dissociation rate of Cas and L744E/R748E GFP-BCAR3 from adhesions could be the result of a specific delay in the dissociation of Cas and mutant BCAR3 from the adhesions, a more generalized stabilization of adhesion proteins in the adhesion complexes, or a reduction in the turnover rate of mutant BCAR3 and Cas. The latter possibility seems unlikely, as ectopic WT and L744E/R748E BCAR3 were found to have similar half-lives (Supplementary Figure S1). Moreover, these half-lives, as well as the half-life of Cas (data not shown), were found to be over 20 h, which is far greater than the 10- to 12-min timespan of the videos used to quantify adhesion disassembly.

To distinguish between the first two possibilities, we examined the adhesion dynamics of another well-established adhesion protein, talin, in the presence of WT or L744E/R748E GFP-BCAR3. Unlike Cas, talin does not associate with WT BCAR3 (Supplementary Figure S2). Live TIRF imaging was performed to visualize adhesion dynamics in cells expressing mCherry-talin and either WT or L744E/R748E GFP-BCAR3, and adhesion turnover was quantified as described above (Figure 4). As before, the incorporation of BCAR3 into adhesions was not dependent on its ability to bind to Cas (Figure 4e, compare bars 1 and 2), but its rate of dissociation from adhesions was significantly reduced in the absence of Cas binding (Figure 4f, compare bars 1 and 2). The rates at which BCAR3 and talin entered and left adhesions were not significantly different (Figures 4e and f, bars 1 and 3). However, as was the case for Cas, the rate at which talin dissociated from adhesions was significantly reduced in the presence of L744E/R748E GFP-BCAR3 (Figure 4f, compare bars 3 and 4). This was also the case for a third adhesion protein, α-actinin (Supplementary Figure S3), which similarly does not interact with BCAR3 (Supplementary Figure S2).

It is important to note that, for all of the adhesion proteins analyzed, the reduced rate at which they dissociated from adhesions in the presence of L744E/R748E BCAR3 was similar to the rate at which the mutant BCAR3 molecule left adhesions (Figures 3f and 4f, and S3F, compare bars 2 and 4). This is consistent with a stabilization of the entire adhesion complex under these conditions, suggesting that a direct interaction between BCAR3 and Cas is required for efficient adhesion complex disassembly and turnover.

Our previous work showed that loss of BCAR3 in breast cancer cells resulted in a reduction of Rac1 activity coincident with an increase in RhoA activity, stress fiber stabilization and slower adhesion turnover.[4] As proper control of adhesion dynamics by BCAR3 required an intact Cas-binding site, we hypothesized that the ability of BCAR3 to promote Rac1 activity may be dependent on its association with Cas. To test this hypothesis, active GTP-bound Rac1 was measured in extracts from BT549 cells expressing WT or L744E/R748E GFP-BCAR3

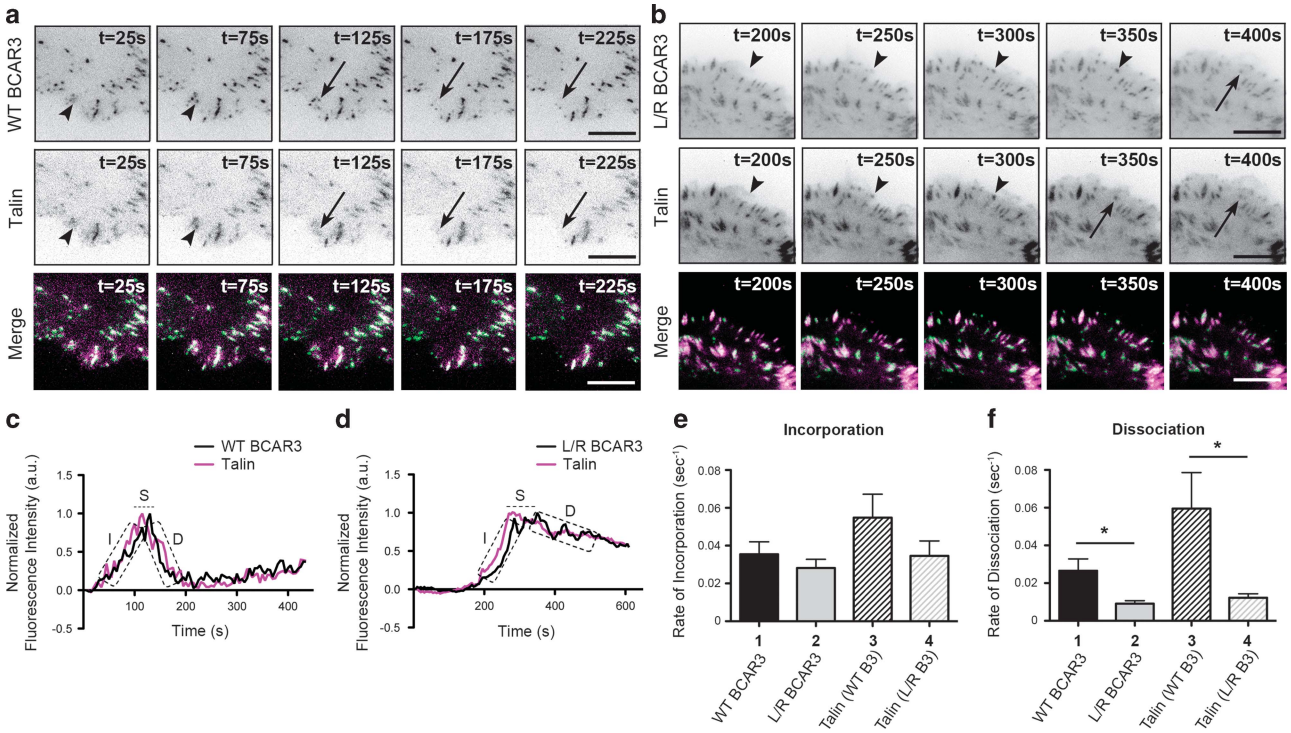

Figure 4. Direct interaction between BCAR3 and Cas is required for efficient dissociation of talin from adhesions. BT549 invasive breast cancer cells were co-transfected with plasmids encoding WT or L744E/R748E (L/R) GFP-BCAR3 and mCherry-talin, incubated for 24 h, and then plated on 2 μg/ml fibronectin-coated glass-bottomed TIRF dishes for 30–40 min before visualizing adhesion dynamics via live-imaging TIRF. (**a**, **b**) Representative time-lapse images show incorporation into adhesions (arrowheads) and dissociation (arrows) of the indicated proteins over the specified time course. Scale bars = 100 μm. (**c**, **d**) Representative fluorescence intensity time tracings of BCAR3 (black) and talin (magenta) present in adhesions from cells expressing WT (**c**) or L744E/R748E (L/R) GFP-BCAR3 (**d**). Dashed boxes/line indicate the incorporation (I), stability (S) and dissociation (**d**) phases of adhesion dynamics. (**e**, **f**) Quantitative analysis of the incorporation (**e**) and dissociation (**f**) rates of WT GFP-BCAR3 (bar 1), L744E/R748E (L/R) GFP-BCAR3 (bar 2), talin co-expressed with WT GFP-BCAR3 (bar 3) and talin co-expressed with L744E/R748E (L/R) GFP-BCAR3 (bar 4). Data presented are the mean ± s.e.m. of ⩾14 adhesions from five separate WT BCAR3/talin or three separate L744E/R748E BCAR3/talin movies generated from three independent experiments. *$P < 0.05$.

(Figure 5). Overexpression of WT BCAR3, but not the Cas-binding mutant, was found to increase Rac1 activity in the cell. Together, these data show that the BCAR3–Cas complex promotes increased Rac1 activation and adhesion disassembly/turnover in breast cancer cell lines.

Direct interaction between BCAR3 and Cas promotes breast tumor cell invasion in 3D and chemotaxis toward serum

Previous studies have shown that BCAR3 promotes breast tumor cell motility and invasion.[2,4] Considering that adhesion turnover is a critical facet of motility/invasion, and that BCAR3 promotes adhesion disassembly through its interaction with Cas (see above), we hypothesized that BCAR3-mediated breast tumor cell invasion and migration would similarly be dependent upon the ability of BCAR3 to bind to Cas. To test this hypothesis, stable MDA-MB-231 cells were generated that express either empty vector (pLKO) or a BCAR3-targeted short hairpin RNA (shBCAR3) (Figure 6A, lanes 1 and 2). The stable shBCAR3 cell lines were then infected with the lentiviral vector pLV-Venus (Figure 6A, lane 3) or shRNA-resistant wobble versions of pLV-Venus WT BCAR3 (lane 4) or the Cas-binding mutant of BCAR3 (L744E/R748E, L/R) (lane 5). The expected Cas-binding capabilities of these molecules were confirmed through analysis of Cas immune complexes (lanes 7–10). Each cell line was seeded in 3D Matrigel cultures to assess whether BCAR3–Cas interactions were necessary for BCAR3-mediated invasion. As has been reported previously for parental MDA-MB-231 cells,[15] control cells formed highly invasive structures when grown in 3D Matrigel culture (Figure 6B, panel a). In contrast, knockdown of BCAR3 resulted in a significant reduction in the percentage of invasive structures observed at day 8 in culture (Figure 6B, panel b, Figure 6C, compare bars 1 and 2). Cells infected with a second shRNA construct that resulted in a less robust knockdown of BCAR3 (Supplementary Figure S4A) exhibited an intermediate invasive phenotype (Supplementary Figures S4B and C). The reduced invasive phenotype exhibited by cells expressing shBCAR3 was rescued by expression of WT BCAR3 protein but not the empty vector or Cas-binding mutant (Figure 6B, panels c–e, Figure 6C, bars 3–5). This requirement for direct BCAR3–Cas binding in BCAR3-mediated invasion was confirmed with a second cell line, HS-578 T (Supplementary Figure S5). To determine the importance of direct binding between BCAR3 and Cas in promoting BCAR3-mediated migration, the MDA-MB-231 cells described above were plated in a modified Boyden chamber and allowed to migrate toward serum for 6 h. Knockdown of BCAR3 resulted in a loss of migration as previously described[2] (Figure 6D, bars 1 and 2). The reduced migration observed in cells expressing shBCAR3 was similarly observed in cells re-expressing the empty vector and the Cas-binding mutant of BCAR3 (Figure 6D, bars 3 and 5) but not in cells re-expressing WT BCAR3 (bar 4). Collectively, these data show that BCAR3 promotes both chemotaxis toward serum and invasion through its interactions with Cas.

BCAR3 is co-expressed with Cas in multiple subtypes of human breast tumors

Considering the strong functional relationship between BCAR3 and Cas in breast cancer cell lines *in vitro,* we next sought to determine whether there was evidence for a similar functional

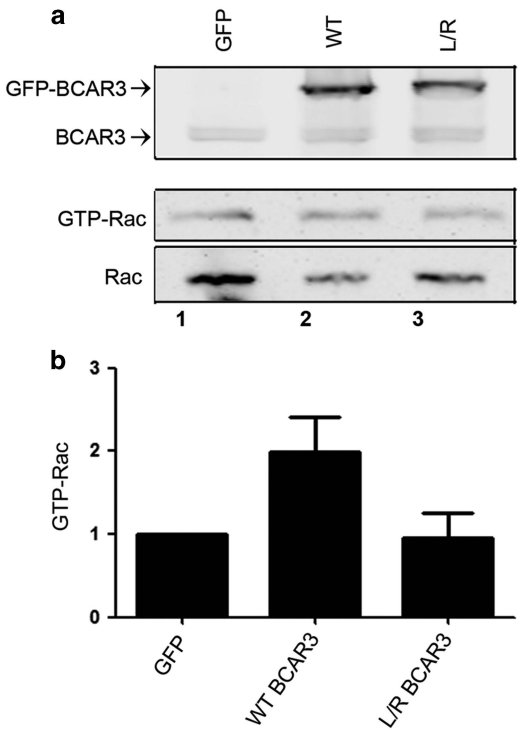

Figure 5. BCAR3–Cas interactions are required for BCAR3-dependent Rac activity. BT549 cells were transfected with plasmids encoding GFP, WT GFP-BCAR3 or L744E/R748E GFP-BCAR3 and incubated for 24 h. Cells were held in suspension for 90 min, then plated on 10 μg/ml fibronectin for 1 h. (**a**) GTP-bound Rac1 was isolated from whole-cell lysates by incubation with PAK-1-binding domain agarose. Bound proteins (middle panel) and total Rac1 (bottom panel) were detected by immunoblotting with a Rac1 antibody, and BCAR3 expression was confirmed with a BCAR3-specific antibody (top panel). (**b**) Quantification of the relative GTP-Rac1 level is shown. Data presented are the mean ± s.e.m. of three independent experiments.

association in human breast tumors. Sequential sections of tumor tissue were stained with hematoxylin and eosin or antibodies recognizing BCAR3 or Cas. BCAR3 expression was found to be low to non-detectable in normal breast tissue (Figure 7, top panels) but upregulated in multiple breast tumor subtypes (bottom 3 panels). Moreover, BCAR3 was found to be co-expressed with Cas in localized regions of tumor tissue (see insets), suggesting that these two molecules may indeed function as a unit in breast cancers.

DISCUSSION

BCAR3 expression is upregulated in invasive breast cancer cell lines and has been shown to promote migration and invasion in these cells.[2,4,16] Work from the Pasquale group demonstrated that direct binding between BCAR3 and Cas is required for enhanced Src activity and Cas phosphorylation.[5] In this study, we sought to further elucidate the importance of BCAR3–Cas complexes in BCAR3-dependent functions, particularly those associated with cell motility and invasion. The functional nature of this protein complex is underscored by our finding that all of the BCAR3 is in complex with Cas in invasive breast cancer cells.

BCAR3 targeting to adhesions is multifactorial

As all of the BCAR3 in BT549 and MDA-MB-231 breast cancer cells is present in BCAR3–Cas complexes, it is formally possible that, in the absence of any perturbation, endogenous BCAR3 enters adhesions together with Cas. However, there must also be Cas-independent mechanisms for adhesion targeting of BCAR3 as ectopically expressed L744E/R748E GFP-BCAR3 readily localized to adhesions despite its inability to associate with Cas (Figure 8a). The SH2 domain has been reported to mediate BCAR3 targeting in mouse embryo fibroblasts through its interaction with protein tyrosine phosphatase α;[3] however, the SH2 domain was dispensable for adhesion targeting in our system. Moreover, the dual SH2/Cas-binding mutant (R171V/L744E/R748E GFP-BCAR3) also localized to adhesions, indicating that there are other focal adhesion-targeting mechanisms that contribute to BCAR3 localization to these sites, at least in the absence of Cas and protein tyrosine phosphatase α interactions. It is unlikely that this targeting activity is a direct consequence of talin and α-actinin, as neither protein was present in WT or L744E/R748E GFP-BCAR3 immune complexes (Supplementary Figure S2). Whether other adhesion proteins are responsible for adhesion targeting of ectopic BCAR3 molecules in these circumstances remains to be determined.

BCAR3–Cas interactions are required for efficient BCAR3-mediated adhesion disassembly, migration, invasion and Rac1 activity

The data presented in the current report provide the first mechanistic insight into how BCAR3 promotes adhesion disassembly and invasion of breast cancer cells. Under conditions in which BCAR3–Cas complexes were able to form (that is, WT BCAR3), we observed rapid dissociation of multiple proteins from adhesions. However, when BCAR3–Cas interactions were blocked (that is, L744E/R748E BCAR3), the rate of adhesion disassembly was significantly reduced. This suggests that the BCAR3–Cas complex contributes to adhesion disassembly. Recent studies have shown that the ability of BCAR3 to induce membrane ruffling/lamellipodia in 2D also requires Cas binding.[5] Data presented in this report expand on these findings by showing that interactions between BCAR3 and Cas are required for the invasive phenotype of breast cancer cells in 3D as well as chemotaxis toward serum. Finally, BCAR3 expression in cells grown on plastic promotes Src-mediated Cas phosphorylation in breast cancer cells, leading to Cas/Crk coupling and Rac1 activation.[2–4,10,11,17,18] We show here that BCAR3-dependent Rac1 activation also requires interaction with Cas. On 3D matrices, Rac1 activity promotes a mesenchymal phenotype, whereas elevated RhoA signaling promotes more rounded cell morphology.[19] It is therefore interesting to speculate that BCAR3–Cas-dependent Rac1 activity may be critical for its ability to promote an invasive phenotype in 3D culture. Whether the adhesion turnover functions of BCAR3–Cas observed in 2D contribute to the BCAR3-dependent invasive phenotype in 3D remains to be determined, particularly as adhesions that form in 2D and 3D may differ significantly in protein composition, dynamics and regulation.[20,21]

The colocalization of BCAR3 and Cas in adhesions suggests that BCAR3–Cas-mediated Rac1 activation is likely to occur at these sites. This activity, coincident with the possible suppression of RhoA in adhesions, could account for the faster rate of adhesion disassembly and turnover observed when WT GFP-BCAR3 and Cas are expressed in the cells (Figure 8b). Although the Cas-binding mutant of BCAR3 was also seen to efficiently localize to adhesions, it failed to promote Rac1 activity. In the absence of BCAR3–Cas interactions (or upon depletion of BCAR3 as was the case in our previous study), we speculate that the inability to locally activate Rac1, together with a possible rise in RhoA-mediated tension, provides the reinforcement necessary to stabilize adhesions and reduce the rate of disassembly (Figure 8c). This model is supported by work from the Lerner group, who showed that deletion of the C-terminus of BCAR3 abrogated both Cas binding and Rac1 activation.[22] They also showed that a mutant of BCAR3 containing a single point mutation in the Cas-binding domain was still able to promote Rac1 activity despite its apparent inability to bind to Cas. It has since been shown, however, that this point mutation may not completely abrogate Cas binding in the cell.[5]

In conclusion, we favor a model wherein BCAR3 promotes Rac1 activation, adhesion disassembly and an invasive phenotype through its binding to Cas, and that interfering with the interaction between these proteins short circuits signaling network(s) responsible for these activities (Figure 8). An alternative explanation for the data presented in this study is that L744E/748E

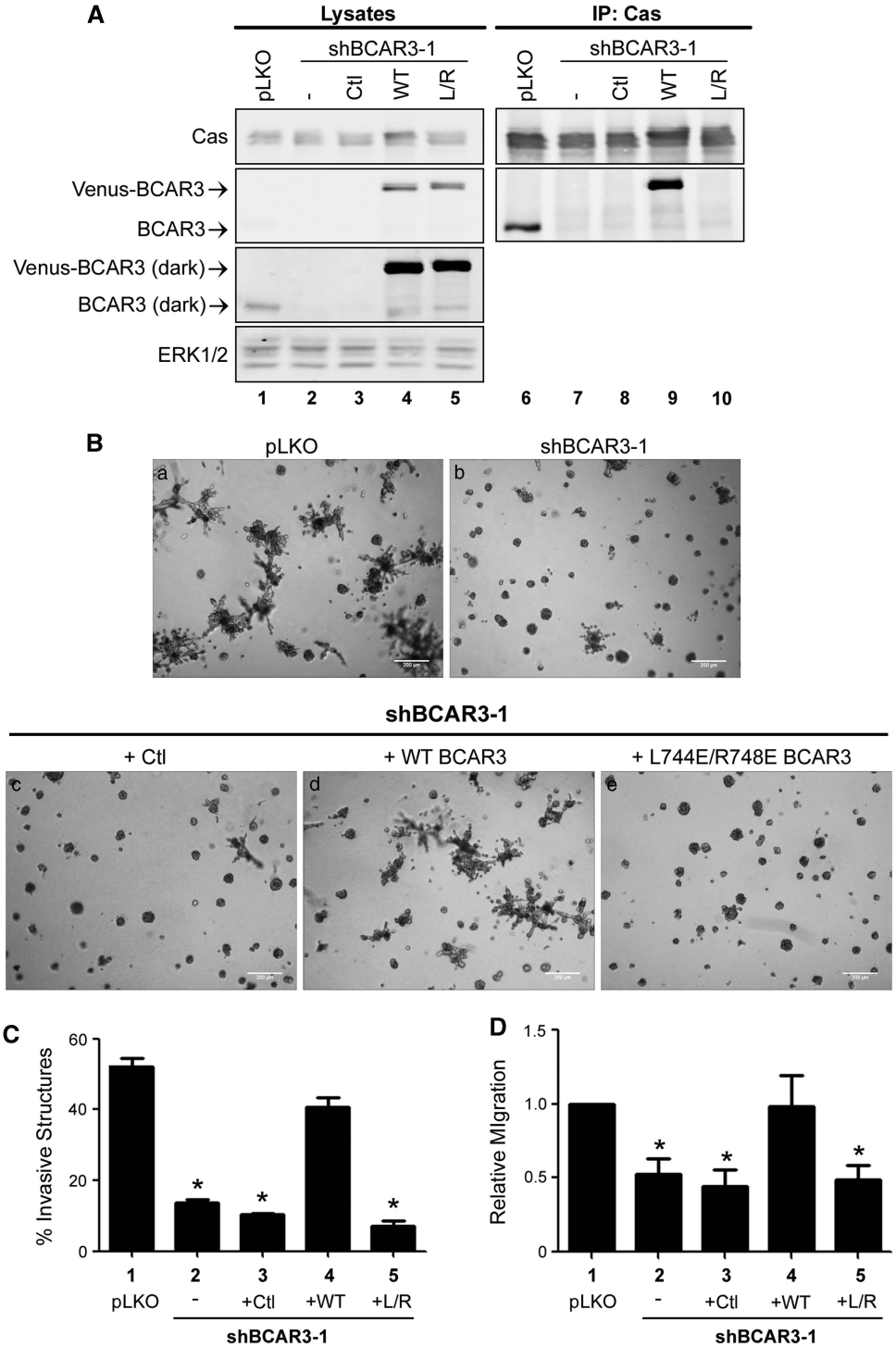

Figure 6. Direct interaction between BCAR3 and Cas is required for invasion of MDA-MB-231 cells in 3D Matrigel culture and chemotaxis toward serum. (**A**) MDA-MB-231 cells stably expressing empty vector (pLKO) or shBCAR3-1 lentiviral constructs were infected with lentiviruses encoding third-base wobble variants of WT Venus-BCAR3 or L744E/R748E (L/R) Venus-BCAR3 or empty vector (pLV-Venus; Ctl). Total cell protein and Cas immune complexes were immunoblotted with antibodies to detect the indicated proteins. Left and right panels are identical exposures from the same film. (**B**, **C**) The cells described in panel **a** were grown in 3D Matrigel culture for 8 days. Representative phase images (**B**) and quantification of invasive structures (**C**) are shown. Data presented are the mean ± s.e.m. of three independent experiments, performed in quadruplicate. Scale bars = 200 μm. (**D**) The cells described in panel **a** were serum-starved overnight and plated (2.5×10^4) in the top of a Boyden chamber (6.5 mm, 8.0-μm Transwell Costar membrane; Corning Inc.). Cells were allowed to migrate toward 10% serum for 6 h and the cells that migrated to the lower chamber were counted. Data presented are the mean ± s.e.m. of seven independent experiments. *$P < 0.05$ relative to pLKO.

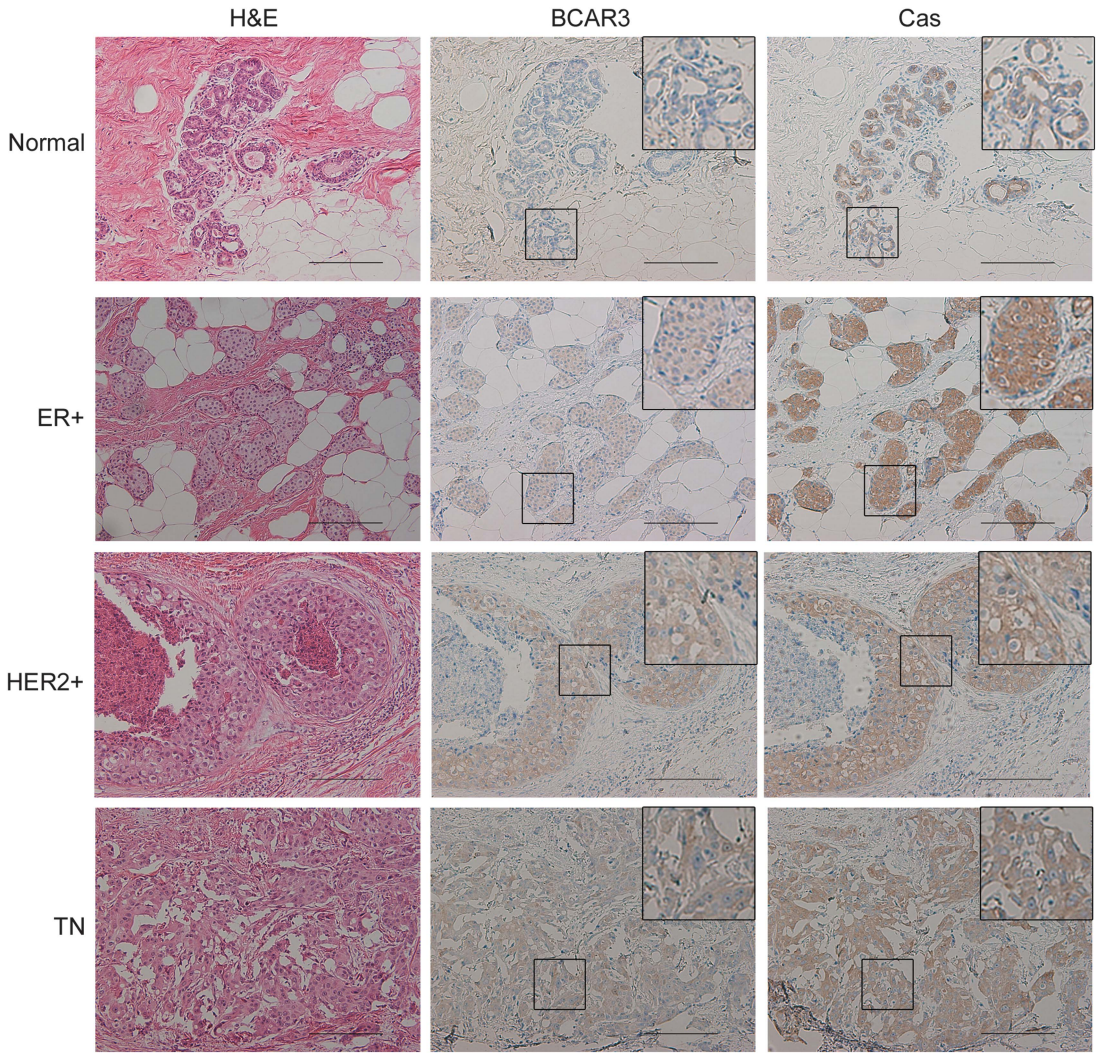

Figure 7. BCAR3 is co-expressed with Cas in multiple subtypes of human breast tumors. Sequential sections of human tissue were stained with hematoxylin and eosin (H&E) (left panels) or immunostained with BCAR3 (middle panels) or Cas (right panels) antibodies. Insets show higher magnifications of the designated areas. Scale bars = 50 μM. ER, Estrogen Receptor; HER2, Human Epidermal Growth Factor Receptor 2; TN, Triple-Negative.

BCAR3 may function independently of Cas to inactivate other molecules/pathways whose functions are critical for these outcomes. We consider this to be unlikely, however, largely because expression of the Cas-binding mutant of BCAR3 phenocopies the effects of BCAR3 knockdown that were reported in our previous study[4] with respect to the adhesion turnover defect and diminished Rac1 activation.

BCAR3–Cas functions as an oncogenic protein complex in invasive breast tumor cells

Despite strong evidence for BCAR3 as a potent regulator of cell adhesion and invasion in breast cancer cells, the fact that a global knockout of BCAR3 fails to cause any major developmental or phenotypic abnormalities at birth[23] indicates that its expression is largely dispensable for morphogenesis. BCAR3 expression is upregulated in invasive breast cancer cell lines,[2,16] and it is in this context that BCAR3 appears to have a critical role in adhesion turnover and invasion. Our finding that the majority of BCAR3 in BT549 and MDA-MB-231 cells is associated with Cas suggests that the function of BCAR3 in these cells is dependent on the BCAR3–Cas complex. This is further supported by the data presented above showing that BCAR3 is co-expressed with Cas in multiple breast tumor subtypes. Together, these data suggest that BCAR3–Cas and/or its downstream effectors may prove to be effective therapeutic targets for tumors that co-express these molecules, particularly because BCAR3 is non-essential for development.

MATERIALS AND METHODS

Antibodies and reagents

Monoclonal antibodies recognizing β-actin (A3854), β-tubulin (T4026), α-actinin (A5044) and talin (T3287) were purchased from Sigma-Aldrich (St Louis, MO, USA). Polyclonal antibodies were obtained from the following sources: BCAR3 (Bethyl Laboratories, Inc., Montgomery, TX, USA; A301-671A); BCAR3 (for immunohistochemistry) (Sigma-Aldrich, HPA014858); GFP (Abcam, Cambridge, UK; AB6673), ERK (Cell Signaling Technology, Inc., Danvers, MA, USA; 9102); Texas red-conjugated goat anti-rabbit (Jackson ImmunoResearch Laboratories, Inc., West Grove, PA USA; 111-075-144); CasB.[24] Additional reagents included fibronectin (Sigma-Aldrich, F1141), EGF (Peprotech, Rocky Hill, NJ, USA; AF-100-15) and Matrigel (Corning Inc., Corning, NY, USA; 354230).

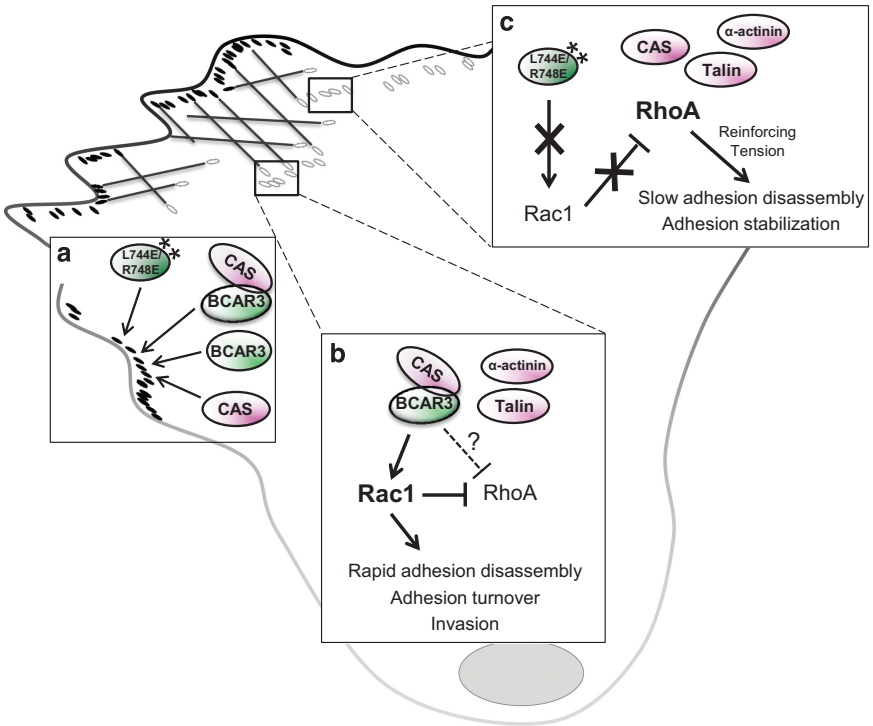

Figure 8. BCAR3–Cas interactions promote efficient adhesion complex disassembly and invasion. (**a**) BCAR3 can efficiently incorporate into adhesions in the absence of a functional Cas binding and/or SH2 domain. (**b**) Under conditions where BCAR3–Cas interactions are enabled (that is, WT BCAR3), rapid disassembly of multiple adhesion proteins is observed. We propose BCAR3–Cas complexes promote localized activation of Rac1 and/or suppression of RhoA under these conditions, therefore initiating rapid adhesion turnover and invasion. (**c**) When BCAR3–Cas interactions are prevented (that is, L744E/R748E BCAR3), local Rac1 activation is diminished, leading to a possible rise in localized RhoA-mediated tension, which provides the reinforcement necessary to stabilize adhesions and slow the rate of disassembly.

Expression vectors

BCAR3 complementary DNA was cloned into the *Eco*RI and *Xba*I sites of pEGFP-C1 (Clontech Laboratories, Inc., Mountain View, CA, USA) to generate pEGFP-BCAR3 (WT GFP-BCAR3). Cas complementary DNA was cloned into the *Xba*1 and *Bam*H1 sites of pm-Cherry-C1 to generate pm-Cherry-Cas.

Mutant R171V, L744E/R748E and R171V/L744E/R748E GFP-BCAR3 proteins were created using the QuickChange II Lightning Site-Directed Mutagenesis Kit (Agilent Technologies, Santa Clara, CA, USA). The following primers were used (changed nucleotides are underlined, and all constructs were confirmed by sequencing): R171V forward: 5′-CGAGATGGTGACTTCCTAGTTGTCGACTCTC TGTCCAGCCCTGGG-3′: R171V reverse: 5′-CCCAGGGCTGGACAGAGAGTCGACA ACTAGGAAGTCACCATCTCG-3′: L744E/R748E forward: 5′-CATGCTGAACCAT GAGGCAACAGCGGAATTCATGGCCGAGGCTGC-3′: L744E/R748E reverse: 5′-GC AGCCTCGGCCATGAATTCCGCTGTTGCCTCATGGTTCAGCATG-3′.

Wobble mutants of BCAR3 were generated in the pLV-Venus vector. WT and L744E/R748E BCAR3 complementary DNA were cloned into the *Not*I and *Spe*I sites of the pLV-Venus vector. Site directed mutagenesis was performed using the QuickChange II XL Site-Directed Mutagenesis Kit (Agilent Technologies) to eliminate targeting by shBCAR3-1 without altering the amino-acid sequence of the resultant BCAR3 protein. The following primers were used: (changed nucleotides are underlined, and all constructs were confirmed by sequencing) shB3wobble1 forward: 5′-CCAGATTTTAACTGCGCT GTCCCGAAAATTGGAACCTCCTCCTG-3′, shB3wobble1 reverse: 5′-CAGGAGGA GGTTCCAATTTTCGGGACAGCGCAGTTAAAATCTGG-3′.

shRNA oligonucleotides targeting BCAR3 and cloned into the TRC2-pLKO-puro vector were purchased from Sigma-Aldrich. Hairpin sequences were as follows: shBCAR3-1 shRNA ID: TRCN0000364816, sequence: 5′-CCG GTAACTGCCCTCTCGCGTAAATCTCGAGATTTACGCGAGAGGGCAGTTATTTTTG-3′, shBCAR3-2 shRNA ID: TRC0000376503, sequence: 5′-CCGGTCGGCATTGCAGTGG ACATTCCTCGAGGAATGTCCACTGCAATGCCGATTTTTG-3′.

Cell culture, invasion, migration and Rac assays

BT549 and MDA-MB-231 cells (American Type Tissue Culture, Manassas, VA, USA) were cultured as previously described.[2,11] HS-578 T cells, generously provided by Dr Kevin Janes (UVA), were cultured in Dulbecco's modified Eagle's medium containing 10% fetal bovine serum, 0.01 mg/ml bovine insulin and 1% penicillin/streptomycin. Cells lines were confirmed to be free of mycoplasma. For 3D culture of MDA-MB-231 and HS-578 T cells, Matrigel (50 μl) was spread evenly on the bottom of eight-well chamber slides. Cells grown in 2D monolayer culture were trypsinized and plated in the chamber slides with Dulbecco's modified Eagle's medium containing 2% (MDA-MB-231) or 10% (HS-578 T) serum, 2% Matrigel, 5 ng/ml EGF, and 0.5 μg/ml (MDA-MB-231) or 1 μg/ml (HS-578 T) puromycin. Cells were grown for 6–8 days with media changes every 4 days. Phase images of representative fields were captured using an Olympus CKX41 (Center Valley, PA, USA) or Zeiss Axiovert 40 CFL inverted scope (Thornwood, NY, USA). Transwell migration assays were performed as previously described,[2] and the cells were stained using Protocol HEMA 3 stain set (Fisher Scientific, Waltham, MA, USA; 122-911). Rac1 assays were performed on BT549 cells transfected with plasmids encoding GFP, WT GFP-BCAR3 or L744E/R748E GFP-BCAR3 as previously described.[4]

Plasmid transfection, lentivirus production and infection

Transfections were performed using Lipofectamine 2000 (Invitrogen, Carlsbad, CA, USA; 11668019) following the manufacturer's specifications.

Lentiviral particles were produced by calcium phosphate transfection of HEK293T cells with a mixture of the transfer vector (pLKO-shBCAR3 or pLV-Venus-BCAR3), packaging vector (psPAX2) and envelope vector (pMD2.G). Medium containing lentivirus was collected 48 h post transfection, filtered through 0.45μm filter and used immediately or frozen at – 80 °C. Cells were infected with lentivirus in the presence of 8 μg/ml polybrene.

Immunoprecipitation, immunoblotting and immunofluorescence

Cells grown in 2D were lysed in ice-cold radioimmune precipitation assay (RIPA) buffer supplemented with protease inhibitors and protein concentrations determined as previously described[2] or in a non-denaturing lysis buffer as described by Wallez *et al.*[5] Immunoprecipitations, immunoblotting and immunofluorescence were performed as previously described.[2]

Live-cell imaging and adhesion turnover analysis

BT549 cells were plated on acid-washed 2 μg/ml fibronectin-coated glass bottom TIRF dishes (MatTek Corporation, Ashland, MA, USA) and incubated for 30–40 min at 37 °C, pH 7.4 in CCM1 media (Hyclone, Logan, UT, USA). Images were captured using an inverted TIRF microscope (1X70; Olympus Life Science, Center Valley, PA, USA) with a 60X objective (±1.5X magnification), a cool charged-couple device camera (Retiga Exi; Qimaging, Surrey, BC, Canada), and heated objective/stage (Bioptechs, Butler, PA, USA). Images were captured every 5 s for 10–12 min using MetaMorph software (Nashville, TN, USA). To quantify adhesion turnover, adhesions at peripheral, protruding edges were manually selected for analysis. Complete fluorescence intensity time tracings for individual adhesions were (1) normalized, (2) corrected for background intensity by subtracting an average intensity value corresponding to a background region away from the cell and (3) plotted. Both the increase (incorporation/assembly) and decrease (dissociation/disassembly) in fluorescence intensity were linear as a function of time on semilogarithmic plots, and rate constants were determined from the slopes of these graphs. Rate constant measurements were obtained for a minimum of 13 individual adhesions on 2–5 cells.

Human breast tumor staining

Sequential sections of breast tissue were received from the University of Virginia Biorepository and Tissue Research Facility (BTRF; IRB#HSR17196). Sections were stained with hematoxylin and eosin or immunostained with BCAR3 or Cas antibodies by the BTRF.

Statistical analysis

Statistical analyses were conducting using GraphPad Prism (San Diego, CA, USA)and the sample size was shown to have adequate power. For the adhesion turnover and invasion analysis, a Kruskal–Wallis one-way analysis of variance and a Dunn's multiple comparison *post-test* were used to compare multiple experimental groups. For migration studies, a one-way analysis of variance and the Dunnett *post-test* were used to compare groups, as the data followed Gaussian distribution and passed a Bartlett's test for equal variance.

CONFLICT OF INTEREST

The authors declare no conflict of interest.

ACKNOWLEDGEMENTS

The authors thank Jessica Zareno for technical assistance with TIRF microscopy and Dr Kristen Atkins for identification and pathological assessment of human breast tumor samples. This work was supported by grants from the NIH (5 T32 CA009109 (ALW, AMC), 1 R01 CA096846 (AHB), 1 F31 CA165703 (ALW), 1 F31 CA130168 (MSG) and GM023244 (ARH)); the Department of Defense Breast Cancer Research Program (BC141713 to AHB); the American Cancer Society (PF-12-136-01-CSM to KEK); and the Women's Oncology Research Fund and NCI Cancer Center Support Grant P30 CA44579 from the UVA Cancer Center. Breast tumor samples were obtained from the UVA tumor bank and stained by the Biorepository and Tissue Research Facility (BTRF).

REFERENCES

1 Riggins RB, Quilliam LA, Bouton AH. Synergistic promotion of c-Src activation and cell migration by Cas and AND-34/BCAR3. *J Biol Chem* 2003; **278**: 28264–28273.
2 Schrecengost RS, Riggins RB, Thomas KS, Guerrero MS, Bouton AH. Breast cancer antiestrogen resistance-3 expression regulates breast cancer cell migration through promotion of p130Cas membrane localization and membrane ruffling. *Cancer Res* 2007; **67**: 6174–6182.
3 Sun G, Cheng SY, Chen M, Lim CJ, Pallen CJ. Protein tyrosine phosphatase alpha phosphotyrosyl-789 binds BCAR3 to position Cas for activation at integrin-mediated focal adhesions. *Mol Cell Biol* 2012; **32**: 3776–3789.
4 Wilson AL, Schrecengost RS, Guerrero MS, Thomas KS, Bouton AH. Breast cancer antiestrogen resistance 3 (BCAR3) promotes cell motility by regulating actin cytoskeletal and adhesion remodeling in invasive breast cancer cells. *PloS One* 2013; **8**: e65678.
5 Wallez Y, Riedl SJ, Pasquale EB. Association of the breast cancer antiestrogen resistance protein 1 (BCAR1) and BCAR3 scaffolding proteins in cell signaling and antiestrogen resistance. *J Biol Chem* 2014; **289**: 10431–10444.
6 Lu Y, Brush J, Stewart TA. NSP1 defines a novel family of adaptor proteins linking integrin and tyrosine kinase receptors to the c-Jun N-terminal kinase/stress-activated protein kinase signaling pathway. *J Biol Chem* 1999; **274**: 10047–10052.
7 Cai D, Clayton LK, Smolyar A, Lerner A. AND-34, a novel $p130^{Cas}$-binding thymic stromal cell protein regulated by adhesion and inflammatory cytokines. *J Immunol* 1999; **163**: 2104–2112.
8 Vervoort VS, Roselli S, Oshima RG, Pasquale EB. Splice variants and expression patterns of SHEP1, BCAR3 and NSP1, a gene family involved in integrin and receptor tyrosine kinase signaling. *Gene* 2007; **391**: 161–170.
9 Mace PD, Wallez Y, Dobaczewska MK, Lee JJ, Robinson H, Pasquale EB *et al.* NSP-Cas protein structures reveal a promiscuous interaction module in cell signaling. *Nat Struct Mol Biol* 2011; **18**: 1381–1387.
10 Cabodi S, del Pilar Camacho-Leal M, Di Stefano P, Defilippi P. Integrin signalling adaptors: not only figurants in the cancer story. *Nat Rev Cancer* 2010; **10**: 858–870.
11 Schuh NR, Guerrero MS, Schrecengost RS, Bouton AH. BCAR3 regulates Src/$p130^{Cas}$ association, Src kinase activity, and breast cancer adhesion signaling. *J Biol Chem* 2010; **285**: 2309–2317.
12 Parsons JT, Horwitz AR, Schwartz MA. Cell adhesion: integrating cytoskeletal dynamics and cellular tension. *Nat Rev Mol Cell Bio* 2010; **11**: 633–643.
13 Webb DJ, Donais K, Whitmore LA, Thomas SM, Turner CE, Parsons JT *et al.* FAK-Src signalling through paxillin, ERK and MLCK regulates adhesion disassembly. *Nat Cell Biol* 2004; **6**: 154–161.
14 Broussard JA, Webb DJ, Kaverina I. Asymmetric focal adhesion disassembly in motile cells. *Curr Opin Cell Biol* 2008; **20**: 85–90.
15 Kenny PA, Lee GY, Myers CA, Neve RM, Semeiks JR, Spellman PT *et al.* The morphologies of breast cancer cell lines in three-dimensional assays correlate with their profiles of gene expression. *Mol Oncol* 2007; **1**: 84–96.
16 Near RI, Zhang Y, Makkinje A, Vanden Borre P, Lerner A. AND-34/BCAR3 differs from other NSP homologs in induction of anti-estrogen resistance, cyclin D1 promoter activation and altered breast cancer cell morphology. *J Cell Physiol* 2007; **212**: 655–665.
17 Klemke RL, Leng J, Molander R, Brooks PC, Vuori K, Cheresh DA. CAS/Crk coupling serves as a "molecular switch" for induction of cell migration. *J Cell Biol* 1998; **140**: 961–972.
18 Akakura S, Kar B, Singh S, Cho L, Tibrewal N, Sanokawa-Akakura R *et al.* C-terminal SH3 domain of CrkII regulates the assembly and function of the DOCK180/ELMO Rac-GEF. *J Cell Physiol* 2005; **204**: 344–351.
19 Yamazaki D, Kurisu S, Takenawa T. Involvement of Rac and Rho signaling in cancer cell motility in 3D substrates. *Oncogene* 2009; **28**: 1570–1583.
20 Harunaga JS, Yamada KM. Cell-matrix adhesions in 3D. *Matrix Biol* 2011; **30**: 363–368.
21 Petrie RJ, Yamada KM. At the leading edge of three-dimensional cell migration. *J Cell Sci* 2012; **125**: 5917–5926.
22 Vanden Borre P, Near RI, Makkinje A, Mostoslavsky G, Lerner A. BCAR3/AND-34 can signal independent of complex formation with CAS family members or the presence of p130Cas. *Cell Signal* 2011; **23**: 1030–1040.
23 Near RI, Smith RS, Toselli PA, Freddo TF, Bloom AB, Vanden Borre P *et al.* Loss of AND-34/BCAR3 expression in mice results in rupture of the adult lens. *Mol Vis* 2009; **15**: 685–699.
24 Bouton AH, Burnham MR. Detection of distinct pools of the adapter protein p130CAS using a panel of monoclonal antibodies. *Hybridoma* 1997; **16**: 403–411.

Supplementary Information accompanies this paper on the Oncogene website (http://www.nature.com/onc)

SUPPLEMENTAL MATERIALS

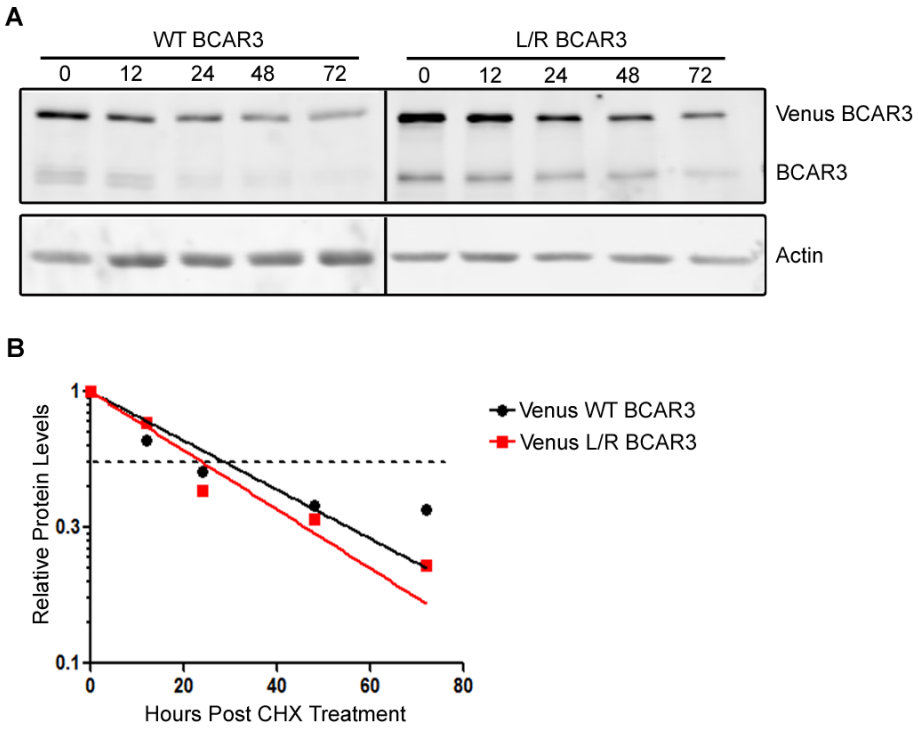

Figure S1. WT and L/R BCAR3 have similar half-lives

(A) BT549 cells were infected with lentiviruses encoding WT Venus-BCAR3 or L744E/R748E (L/R) Venus-BCAR3 and plated in 6-well dishes at 100,000 cells per well. One day after plating, cells were treated with 25μg/ml cyclohexamide (CHX) and lysed at the indicated times. Proteins were immunoblotted with antibodies recognizing the designated proteins. Representative blots are shown. (B) Protein levels from the representative blots were normalized to the 0 hour time point and plotted as an exponential decay nonlinear regression.

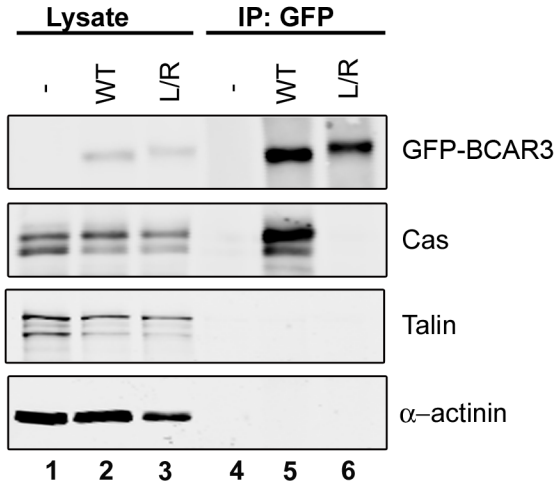

Figure S2. BCAR3 is not in complex with talin or α-actinin

BT549 cells were transfected with plasmids encoding GFP (-), WT GFP-BCAR3, or L744E/R748E GFP-BCAR3 and lysed 24 hours post-transfection. Total cell protein and GFP immune complexes (generated from 50X more protein than the lysates) were immunoblotted with antibodies to detect the indicated proteins.

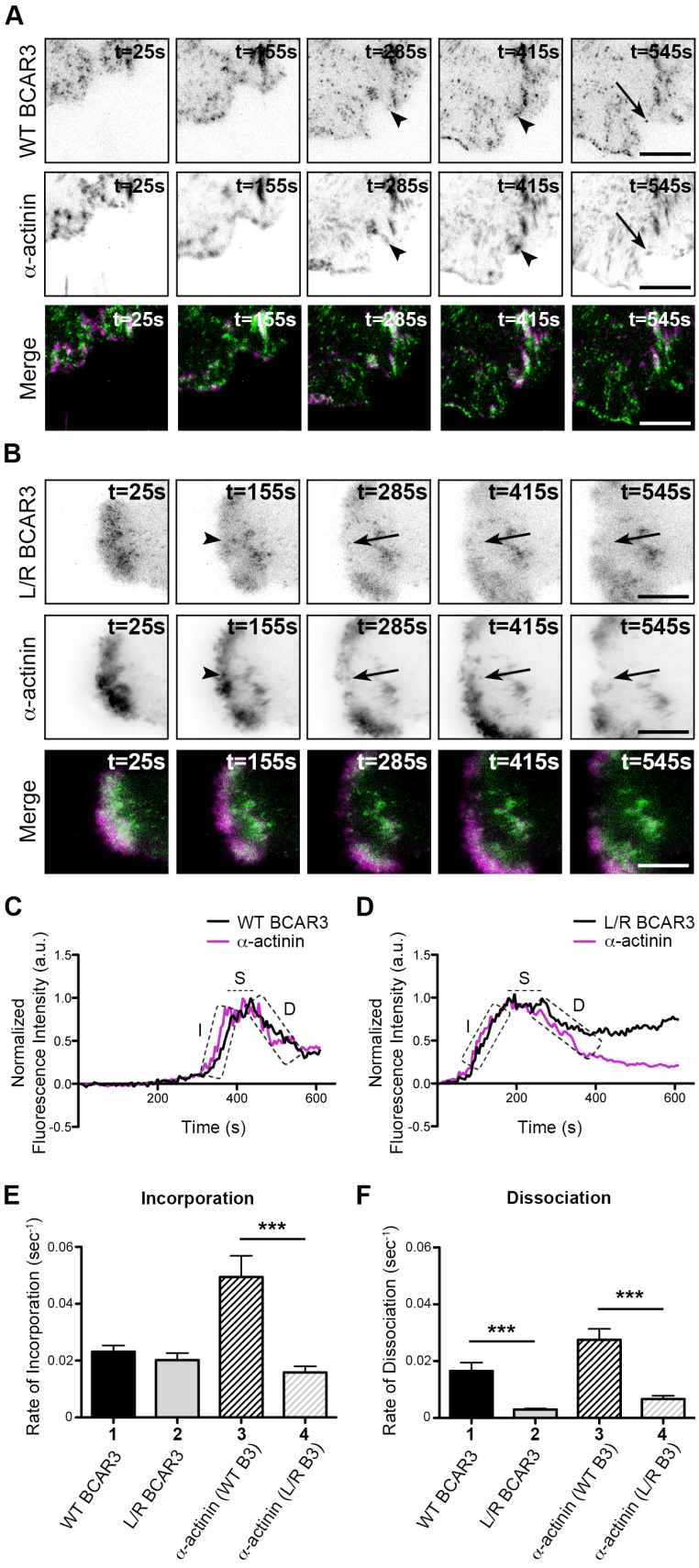
A
WT BCAR3
α-actinin
Merge
t=25s
t=155s
t=285s
t=415s
t=545s
B
L/R BCAR3
C
WT BCAR3
α-actinin
Normalized Fluorescence Intensity (a.u.)
Time (s)
S
D
I
D
L/R BCAR3
E
Incorporation
Rate of Incorporation (sec⁻¹)
***
F
Dissociation
Rate of Dissociation (sec⁻¹)
WT BCAR3
L/R BCAR3
α-actinin (WT B3)
α-actinin (L/R B3)

Figure S3

Figure S3. Direct interactions between BCAR3 and Cas are required for efficient incorporation and turnover of α-actinin in adhesions

BT549 breast cancer cells were co-transfected with plasmids encoding WT or L744E/R748E (L/R) GFP-BCAR3 and mCherry-α-actinin, incubated for 24 hours, and then plated on 2μg/ml fibronectin-coated glass-bottomed TIRF dishes for 30-40 minutes prior to visualizing adhesion dynamics via live-imaging TIRF. (A, B) Representative time-lapse images show incorporation into adhesions (arrowheads) and dissociation (arrows) of the indicated proteins over the specified time course. Scale bars = 100μm. (C, D) Representative fluorescence intensity time tracings of BCAR3 (black) and α-actinin (magenta) present in adhesions from cells expressing WT (C) or L744E/R748E (L/R) GFP-BCAR3 (D). Dashed boxes/line indicate the incorporation (I), stability (S), and dissociation (D) phases of adhesion dynamics. (E, F) Quantitative analysis of the incorporation (E) and dissociation (F) rates of WT GFP-BCAR3 (bar 1), L744E/R748E (L/R) GFP-BCAR3 (bar 2), α-actinin co-expressed with WT GFP-BCAR3 (bar 3), and - -actinin co-expressed with L744E/R748E (L/R) GFP-BCAR3 (bar 4). Data presented are the mean ± SEM of ≥13 adhesions from 4 separate WT BCAR3/α-actinin or 2 separate L744E/R748E BCAR3/α-actinin movies generated from 3 independent experiments. ***, $p<0.001$.

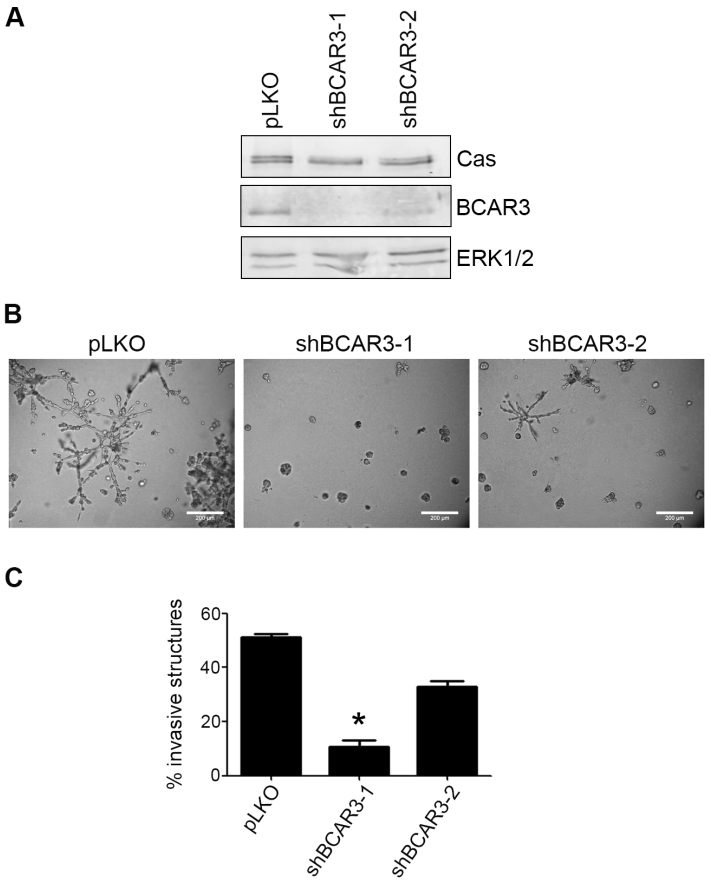

Figure S4. BCAR3 promotes invasion of MDA-MB-231 cells in 3D Matrigel culture

MDA-MB-231 cells stably expressing empty vector (pLKO), shBCAR3-1, or shBCAR3-2 lentiviral constructs were grown in 3D Matrigel culture for 8 days. (A) The cell/Matrigel mixture was collected in 0.25% trypsin, pipetted several times, and incubated for 30 minutes at 37°C. Cells were centrifuged at 150 x g for 3 minutes, washed 1X in DMEM, resuspended in phosphate buffered saline (PBS), and then pelleted by spinning for 3 minutes at 2000 rpm in a micro-centrifuge. The pellet was resuspended in ice-cold RIPA buffer supplemented with protease inhibitors and protein concentrations determined as previously described[2]. A representative immunoblot is shown confirming knockdown of BCAR3 with both shRNA constructs. (B, C) Representative phase images (B) and quantification of invasive structures (C) are shown. Data presented are the mean ± SEM of 3 independent experiments, performed in quadruplicate... Scale bars = 200μm. *, $p<0.05$ relative to pLKO.

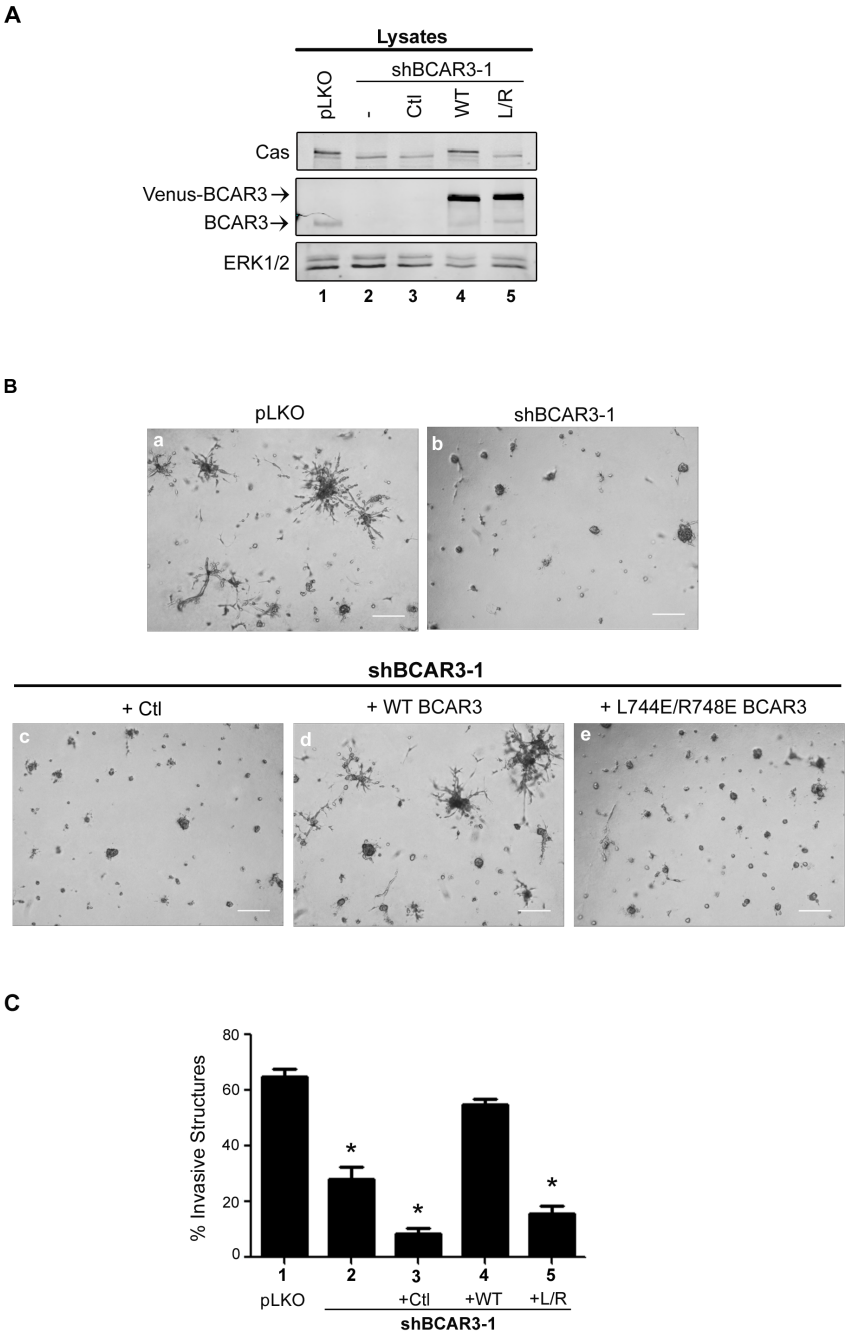

Figure S5: Direct interaction between BCAR3 and Cas is required for invasion of HS-578T cells in 3D Matrigel culture

(A) HS-578T cells stably expressing empty vector (pLKO) or shBCAR3-1 lentiviral constructs were infected with lentiviruses encoding 3rd-base wobble variants of WT Venus-BCAR3, L744E/R748E (L/R) Venus-BCAR3 or empty vector (pLV-Venus; Ctl). Total cell protein was immunoblotted with antibodies to detect the indicated proteins. (B, C) The cells described in

panel A were grown in 3D Matrigel culture for 6 days. Representative phase images (B) and quantification of invasive structures (C) are shown. Data presented are the mean ± SEM of 6-7 replicates per condition from one experiment. Scale bars = 200μm. *, $p<0.05$ relative to pLKO.